Optimal design and operation of reactive distillation systems based on a superstructure methodology

A. Tsatse[1)], S.R.G. Oudenhoven[2)], A.J.B. ten Kate[2)], E. Sorensen[1)*]

1) Department of Chemical Engineering, University College London, Torrington Place, WC1E 7JE London, UK
2) Nouryon, Zutphenseweg 10, 7418 AJ Deventer, the Netherlands

Abstract

A novel methodology for the simultaneous optimisation of design and operation of a complex reactive distillation process, considering a number of process alternatives (e.g. pre-/side-reactor, side-stripper, additional columns etc.), is presented. The methodology is based on a superstructure approach, and a detailed cost-based objective function, solved by MINLP optimisation. The methodology is illustrated using different case studies of industrial interest with varying separation and reaction characteristics. For easy separations, in terms of relative volatilities and boiling points order, a single reactive distillation column is found to be optimal for both fast and slower kinetics. However, when the separation is more challenging (i.e. product is a middle-boiler), the design is more complex, even for fast kinetics, and additional processing units, such as a pre-reactor and/or additional distillation columns, are required to meet the product quality specifications. It is found that the design, i.e. the capital cost, mainly depends on the relative boiling point rankings. For operation, chemical reaction equilibrium is the dominant factor. It is demonstrated, however, that the combined effects of separation and reaction must be considered carefully when designing a reactive distillation process. The liquid holdup has an impact on the reaction performance, and proper choice of holdup can lead to a more flexible design, able to mitigate production failure issues even for slower reactions.

Keywords: reactive distillation, superstructure, optimisation, design

** Corresponding author: e.sorensen@ucl.ac.uk*

1. Introduction

Over the past few decades, there has been an increasing focus on Process Intensification (PI) in an effort to reduce the environmental impact, and to improve the economic performance, of chemical processing plants (Boodhoo and Harvey 2013). Reactive distillation is one of the most well-known Process Intensification examples, and combines reaction and separation into one single unit, thus offering significant capital and operational (including energy) cost savings, obtained through improvements in reaction selectivity and yield (Luyben and Yu 2008, Kiss 2013). However, the combination of the two different phenomena in the same unit makes the design and operation of the process more demanding, mainly due to differences in the operational windows for reaction and separation which do not always fully overlap (Harmsen 2007). In addition, due to the integration of different process functions, the combined effect of uncertainties in design parameters, for instance reaction kinetics, is also expected to be intensified. A very robust yet flexible design is therefore required, which in some cases might involve the inclusion of additional equipment (to perform parts of the processing due to operational window mismatch) in addition to the reactive distillation column.

Although recent research has shed light on many aspects of reactive distillation, the extension of conventional distillation design techniques to reactive systems is still a challenge, and a rigorous methodology for the optimal design and operation of complex reactive distillation processes has not yet been fully established (Wang et al. 2010). Authors who have discussed reactive distillation design and/or operation have generally only considered a single reactive distillation column, and to the best of the authors' knowledge, no contribution to date has considered the simultaneous determination of optimal design and operation of a complex reactive distillation process considering a wide range of process alternatives (for instance pre/side-reactors, additional distillation column(s), side-stripper, side-reboiler etc.). The objective of this work is therefore to provide a novel methodology for determining the optimal design (e.g. total number of stages, existence of additional equipment etc.) and operation (e.g. reflux ratio, flowrates to additional equipment etc.) of a complex reactive distillation process, considering for a first time a large range of process alternatives simultaneously, and to demonstrate the applicability of this methodology for a number of case studies of industrial interest.

Current literature suggests that three categories of methods have so far been successfully applied for the conceptual design of reactive distillation processes: a) graphical methods, b) evolutionary/heuristics-based methods and c) optimisation-based methods. Graphical methods include a range of methods, with the most well-known representatives being the fixed-point technique (Buzad and Doherty 1994, Buzad and Doherty 1995, Mahajani and Kolah 1996) and the residue curve mapping technique (Barbosa and Doherty 1988). Most of those techniques are an extension of conventional, non-reactive, distillation column design methods, for instance, Lee et al. (2000) used short-cut visualisation methods such as Ponchon-Savarit's method and McCabe-Thiele's method to gain design insights for binary reactive mixtures. Graphical methods can be a fast tool for feasibility assessment and preliminary design of a reactive distillation column, however, they are limited by: a) the number of degrees of freedom they can handle; b) their difficulty in visualisation for multi-component reaction systems due to the increased dimensionality; and c) limitations of the underlying assumptions in each case (e.g. VLE, binary mixtures etc.) (Buzad and Doherty 1994, Buzad and Doherty 1995, Mahajani and Kolah 1996, Lee et al. 2000, Lee and Westerberg 2000, Lee and Westerberg 2001). As a result, graphical methods can only be used for initial screening or preliminary design, and not to obtain an optimal rigorous process design.

The second category of methods applied for the design of reactive distillation processes includes evolutionary/heuristic approaches, as firstly developed by Subawalla and Fair (1999) and later extended by other authors (e.g. Tung and Yu 2007, Luyben and Yu 2008). Using these methods, it becomes possible to overcome some of the limitations of the graphical approaches, such as the visualisation difficulty. Moreover, the possibility of also considering column internals (in terms of

catalyst requirements) and economics is offered indirectly by considering reflux ratio and excess reactant requirements, respectively (Subawalla and Fair 1999). These methods are, however, mostly used as a post-design analysis tool as they require a pre-defined process structure to determine process parameters iteratively (Almeida-Rivera et al. 2004). In addition, these methods cannot guarantee optimal column design as no effective heuristics are available to ensure optimality (Huang et al. 2005).

The third category of design methods includes methodologies based on rigorous optimisation, and only this category is capable of considering process design, operation and plant economics simultaneously. However, considering all these factors simultaneously leads to a significant increase in the complexity of this highly non-linear and highly non-convex mathematical problem, and consequently also to increased computational cost. Optimisation methods considered in the literature include Orthogonal Collocation on Finite Elements (OCFE) of equilibrium (EQ) or non-equilibrium (NEQ) reactive distillation models (Seferlis and Grievink 2001) to transform the integer-values stage model to a continuous analogue. The OCFE technique, however, only approximates the kinetically controlled tray-to-tray behaviour and therefore cannot guarantee rigorous results, moreover, its application is challenging for dynamic systems. Another alternative includes the application of memetic algorithms. The latter was used by Urselmann et al. (2011) to find the optimal design for a single reactive distillation process. The method was found to be more rigorous and faster than other algorithms applied so far (e.g. SBB/CONOPT), and the authors claimed that the method could indicate the global optimum. However, the design of efficient memetic algorithms required the development and extensive testing of problem-specific representations, as well as recombination, mutation and selection mechanisms, as stressed by the authors. Other strategies found in literature, such as decomposition of the equation sets (Lima et al. 2006) or a bypass efficiency method on a pseudo-transient model (Ma et al. 2019), can either not guarantee global optimality or show poor numerical performance resulting in practically infeasible solutions as indeed pointed out by these authors.

Another approach for optimisation of reactive distillation is solving the Mixed-Integer Non-Linear (MINLP) optimisation problem, formed by considering all possible alternatives for the optimal design and operation of the process, as well as its dynamic equivalent, thus resulting in a Mixed-Integer Dynamic Optimisation problem (MIDO). As an example, the dynamic problem was solved by Georgiadis et al. (2002) and later by Panjwani et al. (2005), for the optimal design and control of a dynamic reactive distillation column. Nevertheless, both contributions focused only on the structural and control decisions (e.g. total number of stages, controller tuning parameters) of a *single* reactive distillation column, and the methodology was not extended to more complex processes, i.e. including ancillary equipment.

The most rigorous approach for the simultaneous determination of the optimal design and operation of a reactive distillation process is thus solving a complex MINLP optimisation problem. The problem can be formulated in different ways, including using the concept of a superstructure as considered in this work. The first reference to the concept of superstructure was made by Sargent and Gaminibandara (1976), who described a methodology using MINLP optimisation for the optimal design of conventional distillation columns based on minimum cost. In their pioneering work, they solved the MINLP problem using a version of the variable-metric projection method. Their contribution set the foundations for further research on solving this mathematically complex problem, as the authors themselves recognised that more complex systems needed to be considered and that development of techniques which could deal with large-scale non-linear problems was needed.

The first application of MINLP to reactive distillation columns was made by Ciric and Gu (1994) for a non-equilibrium, kinetically controlled, reactive distillation process. The authors took into consideration multiple feed streams, however, also made a number of assumptions, such as ignoring the effect of liquid enthalpies, due to the increased mathematical complexity. The model was solved using Generalized Benders Decomposition (GBD), and it was the first rigorous, tray-by-tray reactive

distillation model. The model was later applied to equilibrium reactions by Frey and Stichlmair (2000). The existence of binary variables (total number of stages, feed stage locations), however, complicated the solution which showed poor numerical performance, thus encouraged the development of alternative solution strategies for the MINLP problem. For instance, Smith (1996) built blocks of reactive flash vessels combined to form a column, whilst Papalexandri and Pistikopoulos (1996) proposed that the problem could be solved as a set of mass and heat transfer modules that integrated to a given network, and both contributions thereby avoided the pre-postulation of a set of unit operations. These approaches were extended by Ismail et al. (2001) to form a block of process alternatives. All the above approaches are, however, nevertheless similar to the classic rigorous tray-by-tray model. Generalised disjunctive programming formulation (Jackson and Grossmann 2001), which uses logic-based outer approximations, is another strategy for the determination of locally optimal design of kinetically controlled reactive distillation columns, based on the general representation and modelling framework suggested by Yeomans and Grossmann (1999) for regular distillation columns. A different strategy, using simulated annealing-based algorithms for the solution of the MINLP optimisation for a NEQ reactive distillation model, was applied by Cardoso et al. (2000), however, their method could not guarantee global optimality as explained by the authors. Recently, Tian et al. (2020) worked towards a more systematic framework, considered the design of reactive distillation systems using a Generalised Modular Representation Framework (GMF), by solving the MINLP formed using GBD. The authors considered a number of factors for the optimal design of the reactive distillation process, such as operability, cost, flexibility etc., however, the methodology included alternating (for the generation of results) between two different simulation tools (GAMS and gPROMS).

Overall, it is generally agreed that MINLP optimisation is required to simultaneously determine the optimal design and operation of a reactive distillation process given the complexity of the problem. Rigorous optimisation becomes even more attractive given the development of increasingly stronger mathematical tools, such as the enhanced Outer Approximation algorithm which is employed in this work (Process Systems Enterprise 2020), which does not have the numerical performance issues faced in the past, and which also enables locating the global optimum for convex problems with reduced computational cost.

In the following, a superstructure of a reactive distillation process including multiple ancillary units will be presented, and it will be shown how the MINLP can be formulated (units included, decision variables etc.) and solved using a systematic methodology. Next, a number of case studies with different key system characteristics (easy/difficult separation, fast/slow reaction, etc.) will be considered to illustrate the methodology, but also to show how the steady-state optimal design and operation of the overall reactive distillation process depend on these key system characteristics. The latter may provide useful insight when considering similar systems.

2. Methodology

The following section describes how the steady-state simulations and optimisation tasks were set up and performed using gPROMS ProcessBuilder v1.3.1 (Process Systems Enterprise 2020) with Multiflash v6.1 (Infochem 2019) on a 3.60 GHz and 32GB RAM Dell Precision 5820 Desktop. To be able to assess the impact of the parameters of the individual chemical systems on the derived optimal reactive distillation designs in general terms, it was decided to use ideal generalized user-defined components instead of a specific real chemical system. This way the parameters that describe a chemical system, such as boiling point rankings, relative volatilities and kinetic constants, can be altered individually in order to investigate different system characteristics, as well as their relative impact both individually and combined. All components therefore have the same basic thermodynamic properties, as shown in Section 4, except for the vapour pressures (and thus, the

boiling points) which were manipulated using their Antoine vapour pressure coefficients to achieve the desired relative volatilities. The methodology used for the manipulation of vapour pressures is presented in Appendix A1. In this work, generic components were considered, therefore using the ideal model is the most appropriate in this case. However, since the methodology is applicable to any components and/or reaction systems, non-ideal behaviour can also be considered (e.g. azeotropes, phase split etc.) using the appropriate thermodynamic model in each case.

The superstructure of the overall reactive distillation process considered is shown in Figure 1 and all decision (manipulated) variables of the units involved, which form part of the optimisation problem, are shown in Table 1. **Error! Reference source not found.**~~Figure 1~~ applies in the cases when the desired product is either the heaviest or the lightest component. If the desired product is an intermediate-boiler then an additional column is needed, and the product will be removed either from DC1 (as bottom stream) or DC2 (as top stream), and the other stream of the additional column will be recycled back to the reactive column. Note that recycles were not included during optimisation for the case studies considered in this work due to current software limitations related to challenging initialisation procedures as will be explained in more detail later (Section 3). However, the recycles could be included in the investigation once the optimal design was found, to further improve the process through steady-state simulations, especially for those case studies where incomplete reactant conversion was observed. The methodology presented in this work can easily be modified to include these recycles when solvers which can tackle the challenging initialisation issues are used and/or become available.

All variables included in Table 1~~Table 1~~ are the decision variables considered in the optimisation. In the following, we shall refer to these as Set ϑ_1 (integer and binary variables) and Set ϑ_2 (continuous variables), respectively. All the decision variables are varied simultaneously such that the design and operation of the process are optimised simultaneously.

The superstructure shown in Figure 1~~Figure 1~~ includes the following units: a pre-reactor (p-CSTR), a reactive distillation column (RDC), a side-reactor (s-CSTR), a side-reboiler (s-reboiler), a side-stripper (s-stripper), a vapour pump-around stream, as well as two distillation columns (DC1, DC2) for further purification of the distillate or the bottom streams of the reactive distillation column, respectively. The units may or may not exist in the optimal process, therefore, the existence of all units depends on the result of the optimisation. The existence of a unit is determined either by the optimal capacity of the unit (e.g. a reactor with zero volume is considered non-existing), or by whether a stream flowing to the unit is selected (a unit with an input stream with an optimal binary variable of 0 is considered not selected).

A pre-reactor was added in the superstructure in order to consider the possibility of selecting the conventional process layout for an equilibrium limited reaction as the optimal solution, i.e. a reactor (p-CSTR) followed by one or more distillation columns (RDC and/or DC1 or DC2). A pre-reactor combined with a reactive distillation column may enhance the reaction conversion for slower reaction kinetics for which a single reactive distillation would be insufficient. A side-reactor (s-CSTR) is considered in order to provide additional liquid residence time to increase reaction conversion and potentially reduce the size of the reactive column (Bisowarno et al. 2004). A side-reboiler (s-reboiler) is considered in order to provide additional heat to improve separation. A vapour pump-around stream (Draw 4, Feed 6) was added to investigate potential benefits in process performance due to internal recycles. This pump-around design has, to the best of the authors' knowledge, not previously been considered, and the exact benefits of this novel pump-around stream on the performance of reactive distillation columns should be further investigated. The addition of a side-stripper (s-stripper) offers the possibilities of: a) elimination of the remixing effect (remixing of the heaviest/lightest component with a middle-boiler at the bottom/top of the column leading to reduced product composition and energy loss) that has been considered in literature case studies (Lee et al. 2012); and b) removal of either an undesired product that could lead to catalyst deactivation in the reactive zone

(Nguyen and Demirel 2011), or a middle-boiling product from a side-draw location; and c) thermal coupling, which may have energy and cost reduction benefits (Wang et al. 2008). Finally, the two distillation columns (DC1, DC2) can be used for further purification beyond that taking place in the reactive distillation column, if required, as well as part of the conventional (reactor plus distillation columns) process.

As shown in Table 1, the optimisation problem contains both integer and binary variables (e.g. total number of stages, stream selection etc.), as well as continuous (e.g. reflux ratio, flow rates etc.) variables, and therefore, the problem is a Mixed Integer Non-Linear Programming (MINLP) optimisation problem. The general mathematical formulation of the MINLP optimisation is as follows (Biegler 2010):

$$\min_{x,\,y} \quad f(x, y)$$

$$\text{s.t.} \quad h(x, y) = 0,$$
$$g(x, y) \leq 0,$$
$$x \in \mathbb{R}^n, \quad y \in \{0,1\}^t$$

where f (x, y) is the objective function (e.g. cost, energy consumption etc.), h (x, y) = 0 are the equality constraints that characterise the performance of the system (e.g. mass balances, energy balances, phase distribution, inherent restricting relationships, kinetic expressions, summation equations etc.), and g (x, y) ≤ 0 expresses the inequality constraints often imposed by the user in order to include process specifications or constraints (e.g. product purity, safety constraints such as distillation column flooding etc.). The real n-dimensional vector *x* represents the continuous variables, such as unit dimensions and flow rates, whilst the t-dimensional vector *y* represents the integer and binary variables which indicate whether a stream, a stage or a process unit, has been selected or not.

In this work, the objective function of the optimisation problem was a production-based Total Annualised Cost (annualised capital and operating cost divided by annual production rate) calculated as shown in Appendix A2. The two constraints imposed on the system were the purity of the desired product, here component D, in the bottom product, $x_{B,D}$, as well as its recovery, $x_{rec,D}$, defined as the amount of component D recovered as product over the total amount of component D actually produced during the reaction. It should be noted that the methodology derived in this work is of course equally applicable to other objective functions or other product specifications. Equally, further ancillary units (e.g. intermediate heat exchangers in reactive zone as suggested by Alcántara-Avila et al. 2015) can also be added to the flowsheet (although will further increase the mathematical complexity of the problem), or removed, thus altering the superstructure considered but not the methodology.

Based on the description above, the mathematical expression of the MINLP formed in this work becomes:

$$\min_{\vartheta_1,\,\vartheta_2} \quad \text{production-based TAC } (\theta_1, \theta_2)$$

$$\text{s.t.} \quad h(\vartheta_1, \vartheta_2) = 0,$$
$$x_{B,D} \geq x_{B,D}^{spec},$$
$$x_{rec,D} \geq x_{rec,D}^{spec},$$
$$\vartheta_2 \in \mathbb{R}^n, \quad \vartheta_1 \in \{0,1\}^t$$

As previously mentioned, ϑ_1 refers to the set of binary and integer variables and ϑ_2 refers to the set of continuous variables. Binary variables can by definition take a value of either 1 or 0 based on

whether a stream is selected or not. Integer variables can also be considered of type 0/1, for instance a column stage can be selected as a feed stage (therefore taking the value 1) or not (value of 0).

In gPROMS ProcessBuilder, the condenser is Stage 1 and the reboiler is stage N_T, and the stage where the vapour boil-up from the reboiler returns to the column (stage N_T - 1) is used as a variable to optimise the total number of stages (N_T) of the column. Figure 2~~Figure 2~~ shows how the total number of stages is set and optimised whilst optimal feed stage locations are found similarly (Viswanathan and Grossmann 1990).

The solver used for the solution of the MINLP problem is OAERAP (Outer Approximation Equality Relaxation Augmented Penalty), which employs an outer approximation algorithm that guarantees global optimality for convex problems (Process Systems Enterprise 2020). The solver first initialises the problem, then solves the fully relaxed NLP problem whilst treating all integer variables as continuous. Next, it solves the master MILP problem which involves linearisation of the objective function and of the constraints at the solutions of all problems considered in the previous steps, and finally solves the primal optimisation problem (NLP), having fixed the integer variables to suggested values from previous iterations. When there is no further improvement in the objective function for a feasible solution, the solver successfully indicates the optimum. For infeasible solutions, the solver terminates. Since the problem considered is highly non-convex, and this type of MINLP problems suffer from the existence of multiple local optima in the continuous sub-problems, the solver still cannot guarantee global optimality, hence different initial guesses were considered to enhance the possibility of locating the global optimum, as will be explained in the following.

3. Optimisation strategy

The methodology developed in this work for the optimisation of the reactive distillation superstructure is illustrated in the tree diagram in Figure 3~~Figure 3~~. The first three steps consider the initialisation of the superstructure flowsheet. We would like to stress the importance of a careful initialisation procedure for a flowsheet of such a high level of complexity due to the number of units included, and therefore large number of degrees of freedom. In addition to the complexity of the process, a large set of equations needs to be solved for the calculation of the cost-based objective function. The latter could either be based on the built-in gPROMS ProcessBuilder cost calculations or on user-defined cost calculations as considered in this work, although adding the same level of complexity in both cases. For optimisation based on a cost-based objective function using gPROMS, a Saved Variable Set (SVS) with initial guesses for all variables excluding costing is needed as the solver cannot otherwise initialise the cost calculation section as this requires a simulation to already have been performed. In this work, for the successful initialisation of the problem, including both the flowsheet and the cost calculation, a three-step strategy is employed (steps 1 to 3 in Figure 3), where the flowsheet is first gradually introduced and initialised without including the cost calculation, then repeated with the cost calculation based on the SVS. The next step is the actual optimisation of the steady-state process (step 4), which is repeated a number of times using different initial guesses (step 5) to increase the possibility of locating the global optimum. In the following, each step of the methodology will be considered in detail.

Step 1: Flowsheet set-up

First, all process units (distillation columns, reactors etc.) considered (including their feed streams) are added into the flowsheet, one by one starting with the reactive distillation column. Adding one unit at the time until the superstructure is complete was found to be the most efficient way to initialise the superstructure, as otherwise, adding all units simultaneously would in most cases create convergence issues. Setting up the reactive column first and then adding the two reactors (in any order) was found to be the most successful. Next, the side-reboiler, side-stripper and vapour pump-around stream were added in the flowsheet in this order. Finally, the top and bottom distillation columns were added one at a time to ensure that suitable column specifications were given. For the

case studies shown later using gPROMS ProcessBuilder, the "*Distillation column*" model was selected for the reactive and non-reactive distillation columns. For the pre/side-reactors, the "*Reactor stirred tank*" model was considered. For the side-reboiler, the "*Evaporator kettle*" model, whilst for the side-stripper, the "*Distillation column reboiled*" model was used. "*Stream duplicators*" and "*Stream selectors*" were also added in the flowsheet to represent the selection between many alternative streams feasible. Finally, "*Source material*" and "*Sink material*" models were added to model the feed inlets and product outlets, respectively.

Step 2: Flowsheet initialisation, excluding economics

Having set up the superstructure flowsheet, initial values for all units included are required, and this was done one unit at the time as explained in step 1. If the flowsheet could not converge after the addition of a unit, the initial values of the latter were manually adjusted to help the simulation initialise. This strategy was particularly helpful for the units which are connected to the reactive distillation column through a side stream, as the location of the side streams was often a reason for simulation failures. The side stream locations were then varied until the simulation could initialise without any issues. In other cases, when initialisation failures occurred with the addition of a unit, changing the specifications of the unit that the new unit was interacting with was more helpful instead of varying the specifications of the unit added last. It should be noted that the initial values thus manipulated have no impact on the final optimal solution and thus only provide a stable starting point for the optimisation.

Closing recycling loops in the superstructure is numerically very demanding, and built-in initialisation procedures for recycle loops are often not adequate. Accurate initial guesses, in particular for temperature, pressure and exact composition of the recycle stream(s), may need to be provided for the flowsheet to converge. However, even using this strategy did not always lead to a successful flowsheet optimisation including recycle loops when using gPROMS ProcessBuilder. As a result, to ensure consistency across all the case studies considered, recycle streams were not considered during optimisation for the cases presented in this work. However, the recycles could be reintroduced in the investigation once the optimal design was found, to further improve the process through steady-state simulations, especially for those case studies where incomplete reactant conversion was observed. This procedure is clearly not optimal, but was the only option with the current software limitations.

It is of course possible for the optimisation to deselect one of the current existing units and to select other units not currently used. It is important to note that, although some units may not exist in the initial superstructure, they must nevertheless still be configured. If not all models are specified, then the overall flowsheet model will not be able to initialise. For instance, even though a stream that goes into a distillation column, e.g. DC1, was not initially selected, meaning that DC1 did not exist, the model of DC1 must still be configured. In other words, initial guesses for its total number of stages, feed stage location, reflux ratio and distillate flow rate must still be provided.

The steady-state model is first initialised without the cost calculation included. Following successful initialisation, a Saved Variable Set (SVS) that includes the steady-state values of all variables is created in the gPROMS ProcessBuilder results folder and copied to the working folder to provide the initial guesses required for the next step which includes the cost calculation.

Step 3: Flowsheet full initialisation, including cost calculation

After the initialisation of the superstructure excluding the cost calculation, the equations needed for the cost evaluation are added in the model. Although gPROMS ProcessBuilder has a built-in costing tool, in this work the cost calculation was added manually via the gPROMS language section. The gPROMS costing tool was not chosen in order to enable the use of a more detailed cost function, which

can more easily be adjusted to meet user requirements. The Saved Variable Set (SVS) obtained from step 2 was used to initialise and solve the flowsheet, now including the calculation of cost.

Step 4: Set-up and execution of MINLP optimisation

To set up the MINLP optimisation, the objective function, decision variables and user-imposed constraints are selected, and in this work, this is done via a ProcessBuilder optimisation entity. For the decision variables, in addition to their corresponding initial values and variable range, the type of each variable is selected, which for this work is either continuous or discrete (the latter in gPROMS ProcessBuilder are named Special Ordered Set). The range of the continuous variables during optimisation should be considered carefully. For instance, the mass balances for the distillation column must be considered in order to ensure that the range provided for the optimisation of the distillate rate is in agreement with the amount expected from the top of the column (i.e. process capacity). If the range of the distillate rate exceeds or limits the amount that can be removed from the top of the column then it is possible that optimisation will fail or will hit the upper or lower bound of the variable. When the entity is fully configured, the optimisation description is complete.

Step 5: Investigation of sensitivity of optimal solution to initial guesses

After the optimisation problem has been set up, a few steps are required in order to ensure that the solver can indicate a solution and establish that the solution found is the real global optimum. For instance, the length of the reactive zone in the reactive distillation column must be considered as the length cannot be directly manipulated in gPROMS ProcessBuilder for every optimisation iteration. For instance, when the initial guess for the total number of stages for the reactive distillation column was say 50, with stages 2-49 being in the column section and thus reactive, then during optimisation, those 48 reactive stages were not adjusted by ProcessBuilder to match the current total number of stages for that optimisation iteration. In other words, ProcessBuilder would continue to calculate the reaction conversion also for stages that were currently not present. To get around this issue, a manual adjustment of the reactive zone was necessary to ensure that the final total number of stages matched the reactive zone considered during initialisation. To deal with this, when the optimiser indicated a much lower number of stages compared to the number considered during initialisation, a new initialisation was configured with a lower number of stages, i.e. including fewer reactive stages to minimise the difference between the two variables during the iterations, and then re-optimised. This manual procedure is clearly inefficient but is currently the only way that this problem can be solved using ProcessBuilder and it would apply to reactive columns with multiple reactive zones as well. The latter option, although possible, is not considered in this work as non-/auto-catalyzed reactions are considered.

In some cases, optimisation was difficult to complete. For instance, ProcessBuilder was able to solve the inner NLP problem but when it came to the outer MILP problem, the optimiser could not converge and failed to find a solution. In such cases, the optimal NLP point (i.e. the latest successful iteration) could be located at the point just before the optimiser failed and this intermediate solution could be re-initialised and then re-optimised, to reach the final optimal solution. This strategy was found to be successful for those case studies in this work which included reactive columns with a large number of trays and/or designs with additional equipment.

Furthermore, the solver used in this work can only guarantee global optimality for convex problems. The MINLP problem developed in this work is highly non-convex, therefore global optimality is not guaranteed. To increase the confidence that the best solution has indeed been found, the optimisation is considered multiple times starting from different sets of initial guesses to ensure that the same optimum is found in all cases, i.e. that the solution is likely to be the global optimum. In cases where the optimisation results only varied slightly in terms of the value of the objective function and the values of the optimal design and operational parameters, the optimal solutions were considered

equivalent. In this work, this was considered valid when the difference in the objective function value was less than 0.01 €/kg, which is more than sufficient from an industrial point of view.

4. Case studies

The optimisation of the reactive distillation superstructure outlined in Section 2 and illustrated in Figure 1~~Figure 1~~ was performed for a number of case studies for a quaternary system of components A and B which react towards components C and D, in order to demonstrate how the methodology described in Figure 3~~Figure 3~~ can be applied, as well as to explore the optimal solutions for different conditions. Component C was considered to be aqueous (i.e. water) whilst components A, B and D were considered to be organic compounds, based on esterification systems often considered in the literature for reactive distillation studies (e.g. Luyben and Yu 2008). The case studies were selected based on their industrial relevance, in collaboration with the industrial partner. The impact of separation and reaction parameters on the optimal design and operation of different systems was also considered in order to evaluate the relative impact of separation vs kinetics on a reactive distillation process. In particular, the case studies consider systems of different separation difficulty, as well as different kinetic characteristics, to identify under which conditions the reactive column, and/or the associated ancillary units, would be needed.

Formatte

The separation difficulty is defined in terms of the relative volatilities between the components. Five different systems of varying separation difficulty (α_{CA}, α_{AB}, α_{BD}) were considered (Table 2~~Table 2~~), and for each, fast and/or slower kinetic expressions were investigated (Table 3~~Table 3~~). For all the case studies, the components were considered of equal density (900 kg/m^3) and of equal molecular weight (50 g/mol). In addition, the boiling point of the heavy reactant, component B, was also assumed to be fixed (413 K at 1 atm) and all other volatilities were calculated using the heavy reactant as the reference (see Appendix A1).

A quaternary system in which the following non/auto-catalysed reversible reaction occurs in the liquid phase is considered, and applies to all units where reaction is present (e.g. RDC, p-CSTR etc.):

$$A + B \rightleftharpoons C + D$$

The kinetic expressions for the forward (f) and backward (b) reaction rates are the following:

$$r_f = k_{f0} e^{-Ea_f/RT} C_A C_B$$

$$r_b = k_{b0} e^{-Ea_b/RT} C_C C_D$$

where the reaction rates, r_f and r_b, are expressed in kmol/(m^3·s); the pre-exponential kinetic factors, k_{f0} and k_{b0}, are expressed in m^3/(kmol·s); the activation energies, E_{af} and E_{ab}, are expressed in kJ/kmol (assumed to be 80 kJ/mol for both directions); and the concentration of component i, C_i, is expressed in kmol/m^3. The heat of reaction was assumed to be negligible (which is typically the case for equilibrium limited reactions such as esterifications or etherifications), thus the activation energy is the same for both reaction directions and chemical equilibrium (K_{eq}) and equilibrium concentrations are independent of temperature. It is of course possible to consider different reaction schemes/mechanisms within the methodology presented.

For systems I, II, IV and V of Table 2~~Table 2~~**Error! Reference source not found.**, the following boiling point ranking applies: $T_C<T_A<T_B<T_D$, which is the situation when the reactants are the middle-boilers and the two products are removed from the top and bottom of the column, respectively. For system III, the boiling point ranking is alternating: $T_C<T_A<T_D<T_B$, and there is a different boiling point order between one reactant (high-boiler B) and one product (middle-boiler D). All five systems (in terms of

boiling point ranking) apply to a range of industrial processes. These could for instance be the production of ethyl/methyl acetate (Tang et al. 2005) for System III boiling point rankings whilst industrial examples for Systems I, II, IV and V could be the production of isopropyl ester (Reepmeyer et al. 2004), n-butyl acetate or amyl acetate (Luyben and Yu 2008). The methodology presented will of course also apply to real systems such as these.

Fast and slow kinetics, characterised by different chemical equilibrium (K_{eq} was used to calculate k_{b0} based on k_{f0}, $K_{eq}=k_{f0}/k_{b0}$) were considered in combination with the relative volatility systems (Table 2~~Table 2~~), resulting in the case studies given in Table 3~~Table 3~~. Three different values for chemical equilibrium were considered: 0.184, 2.25 and 81 which correspond to a single pass reaction conversion of 0.3, 0.6 and 0.9, respectively. In addition, the values of k_{f0} were calculated based on the time needed to reach 90% conversion in a batch reactor, neglecting the backward reaction. Times considered were 15 min ($k_{f0}=8.41\cdot10^6$ $m^3/(kmol\cdot s)$), 60 min ($k_{f0}=2.1\cdot10^6$ $m^3/(kmol\cdot s)$) and 120 min ($k_{f0}=1.05\cdot10^6$ $m^3/(kmol\cdot s)$). The values of the reaction parameters, as well as relative volatilities, were selected based on industrial interest.

The following assumptions are made:

1) Thermodynamic vapour-liquid phase equilibrium is assumed on every stage of the distillation columns. For a trayed column, this is a reasonable description of the system physics and has been found to sufficiently describe the behaviour of most real columns (Halvorsen and Skogestad 2000).
2) Perfect mixing in the liquid and vapour phases was assumed (Halvorsen and Skogestad 2000). This assumption is considered valid at small or medium scales as for the case studies considered (Vora and Daoutidis 2001), however, at industrial scale, detailed mass transfer and reactant conversion analysis would be required to describe the process more accurately.
3) Constant relative volatilities were assumed throughout the columns (reactive and non-reactive). This is a commonly made assumption (Sargent and Gaminibandara 1976) which is reasonable for close to ideal systems when the temperature range in the column is not very wide and for when generic components, whose behaviour is not already known, are considered, as in this work.
4) Pressure drop was considered negligible for this work, but could easily have been included but would then increase the size of the optimisation problem further.
5) Reaction occurs only in the liquid phase, which holds for many reactions e.g. esterification systems for which reactive distillation has been successfully applied (Luyben and Yu 2008).
6) All column stages (stages 2 to N_T-1) were considered reactive in the reactive distillation column (RDC), with the same liquid holdup per tray.
7) There was no heat loss or gain from the environment in any of the equipment used, therefore, all models were assumed to operate adiabatically.

For all case studies considered, the initial flowsheet included the reactive distillation column (RDC), as well as the side-stripper (s-stripper), the vapour pump-around stream and the top non-reactive distillation column (DC1). The pre- and side-reactors, as well as the side-reboiler and bottom non-reactive distillation column (DC2), were included in the flowsheet, however, were assumed to not participate in the superstructure process initially (Table 4~~Table 4~~). As mentioned previously, these units must also nevertheless be part of the initialisation, even if non-existing (i.e. to avoid zero flows etc.).

The pressure was fixed at 1 atm throughout the process as optimising pressure would further increase the already high complexity of the problem. However, as column pressure impacts both on reaction kinetics and separation performance, it would be interesting to include this in the optimisation as a decision variable in future contributions. The feed streams to the overall system were one stream of

reactant B (Feed 1) of flow rate 12.6 kmol/hr, and one stream of reactant A (Feed 2) of the same flow rate (1:1 feed molar ratio). These feed flow rate values were selected as they correspond to 5 ktn/year of product D when full reactant conversion applies, which is an industrially relevant production rate. The feeds were assumed to be at the corresponding boiling points. In addition, the liquid holdup of the reactive distillation column was fixed at 0.1 m^3/reactive tray (holdup is specified for reactive columns only in gPROMS ProcessBuilder).

A clarification is in order regarding the choice of liquid holdup value. Liquid holdup could not be used as an optimisation variable in ProcessBuilder, therefore it was kept at a fixed value, however, the impact of this choice was investigated separately (see Section 5.2). For case studies with more challenging separation and/or reaction characteristics, the choice of liquid holdup is expected to impact on the optimal design as a higher residence time may be needed, however, a fixed value was selected for all case studies for consistency and comparison. The value of 0.1 m^3/reactive tray was chosen in order to provide reasonable residence time for slow reactions and at the same time avoid very large tray weir heights and column pressure drop (for industrial scale scenarios where pressure drop is not ignored). Using a column with a diameter of 1 m (based on the flooding limit of 80% using Fair's correlation) as an example, which is reasonable given the process flow rates considered, the holdup will provide adequate residence time for reasonably slow kinetics using a tray weir height of approximately 12 cm, which is sensible from an internals' point of view.

As previously mentioned, two inequality constraints were imposed on the optimisation problem, bottom product purity, $x_{B,D}$, required to be at least 99 mol%, and bottom product recovery of the main component (component D), $x_{Rec,D}$, required to be at least 90%.

5. Results

In this section, the optimisation results for the case studies considered will be presented and discussed. More specifically, the optimal designs will first be discussed in terms of optimal cost, followed by a more detailed analysis for all case studies, categorised based on their relative volatility system. In parallel, the behaviour of the optimal systems will be explained, based on their temperature, composition and chemical driving force profiles. Then, a generic discussion with regards to the optimal designs based on their reaction and separation characteristics will take place, leading to the development of design guidelines and to a 3-D figure illustrating the optimal results, mainly in terms of the units involved. Investigations of the impact of liquid holdup and total number of stages on the optimal design and optimal cost, respectively, will follow.

5.1 MINLP optimisation results

Using the methodology described in Section 2, the optimal results presented in Table 5~~Table 5~~ and Table 6~~Table 6~~ were obtained for the case studies given in Table 3~~Table 3~~ with initialisation values as shown in Table 4~~Table 4~~. All steady-state simulations required for steps 1 to 3 of the methodology typically took about 2-120 s CPU time whilst the optimisation tasks took approximately 200-3000 s CPU time depending on the case study considered, as the number of model equations involved was relatively large and in the order of thousands. Optimisations which indicated the existence of additional units were typically slower, requiring more time (up to 1 hr) due to the increased complexity of the problem.

Formatte
Formatte
Formatte

As previously mentioned, the optimisation problem considered is highly non-convex, thus global optimality cannot be guaranteed. The optimisation tasks were therefore repeated with different initial guesses to ensure that the optimum found was indeed the overall optimum (step 5 of the methodology). In all cases considered, starting from different initial guesses still resulted in the same optimal results in terms of the units required, as well as very similar results in terms of total number of stages, feed stage locations and operational parameters, with only very small absolute differences in the objective function (order of 10^{-3} €/kg) which was below the tolerance used (10^{-2} €/kg). As a

result, it is concluded that, particularly from an industrial point of view, all the optimal solutions found for each case study are equivalent since their objective function is almost identical and their optimal parameters are very similar.

5.1.1 Evaluation of optimal costs

A comparison of the annualised capital and operating costs for the optimal designs is presented in Figure 4. Case studies 10 and 11 have significantly larger capital cost than any of the other case studies, mainly due to the large size of the reactive distillation column (85 and 78 stages, respectively), as well as the existence and size of the two additional distillation columns. The next most expensive in terms of capital cost is Case study 9, due to the presence of the pre-reactor, the reactive column and the two non-reactive columns. Case studies 7, 8, 12 and 14 also have reasonably high capital cost due to the existence of the pre-reactor (Case study 8) or the large reactive column (Case studies 7, 12 and 14) required, respectively. For the rest of the cases, capital cost is relatively similar since the designs are based on a single reactive column.
The operating cost is similar for most case studies, since the main contributor to the operating cost is feedstock which is fixed at $10.08 \cdot 10^6$ (€/yr). The operating cost for Case study 10 is the highest and Case study 11 the second highest, due to the high reboiler duty of the two additional distillation columns, the more expensive waste treatment due to unreacted A and B, as well as the higher maintenance cost which is a function of the capital cost. For larger scales, as capital cost scales with a factor of 0.6 whilst operating cost scales linearly, it is expected that increasing capital cost will impact less significantly (comparing to operating cost) on the objective function, and most likely indicating the requirement of additional (side) equipment instead of additional operating cost.

An indicative breakdown of the capital (Figure 5a) and operating (Figure 5b) cost for Case study 8 (pre-reactor and reactive distillation) is presented in Figure 5~~Figure 5~~ as an example. From Figure 5a it can be seen that the largest contributions to the capital cost stems from the reactive column shell, followed by the pre-reactor. Feed cost is the main contributor to the operational cost (Figure 5b), with reboiler duty and maintenance the next two significant operating cost factors. Waste cost is negligible for this system since there is negligible organic waste from the top stream, assuming that product C is water (see Appendix A2 for more information on this assumption).

In the following, a more detailed analysis of the optimal results, as presented in Table 5~~Table 5~~ and Table 6~~Table 6~~, is performed. Also, as the chemical reaction is a function of temperature, the temperature conditions in the reactive distillation column will have an impact on the progression of the reaction. Pressure can also impact on boiling points and reaction rates, however, its impact is not relevant in this work as pressure was considered constant throughout the column. To gain further insight into the optimal results obtained above, it is therefore interesting to consider temperature profiles, and the associated composition and chemical driving force profiles, in some detail. Figure 6~~Figure 6~~ presents the temperature profiles, and Figure 7~~Figure 7~~ shows the corresponding liquid phase composition profiles, for the optimal reactive distillation column designs for all case studies. In addition, Figure 8~~Figure 8~~ shows the chemical driving force (forward reaction rate divided by backward reaction rate) for all case studies. Feed stages are symbolised with a different marker symbol.

5.1.2 Process flowsheets and profiles

System I (Case studies 1-5)

It can be seen from Table 5~~Table 5~~ that the case studies considering System I (Case studies 1, 2, 3, 4 and 5, i.e. relative volatilities of 2-1.5-2 for α_{CA}-α_{AB}-α_{BD}, respectively) needed only a single reactive column to meet the product specifications whilst minimising the objective function. Also, for these five case studies, the faster the kinetics, the lower the total number of stages and the reflux ratio, and therefore also the lower the production-based TAC ($k_{f0}=8.41 \cdot 10^6$ (m^3/(kmol·s)) and $K_{eq}=81$ with corresponding TAC of 2.073 €/kg; $k_{f0}=2.1 \cdot 10^6$ (m^3/(kmol·s)) and $K_{eq}=2.25$ with corresponding TAC of 2.140 €/kg; and $k_{f0}=1.05 \cdot 10^6$ (m^3/(kmol·s)) and K_{eq} = 0.184, 2.25 and 81, respectively, with

corresponding TAC of 2.231, 2.178 and 2.168 €/kg, respectively). The impact of K_{eq} is limited, as Case studies 3 (K_{eq}=2.25) and 5 (K_{eq}=81), which have the same k_{f0} ($1.05 \cdot 10^6$ (m^3/(kmol·s)), have very similar designs and therefore, similar optimal TAC (2.178 and 2.168 €/kg, respectively). To demonstrate the benefits from process intensification, the optimal TAC for the conventional process (reactor followed by non-reactive distillation columns) for Case study 1 was found to be 2.424 €/kg, i.e. 16.9 % higher than the reactive distillation configuration (detailed results not shown).

For Case studies 1-5, the temperature profiles in Figure 6 indicate a gradual increase in temperature from the top to the bottom of the column, where feed stages only slightly disrupt the smooth increase. The gradually increasing temperature profile is due to the favourable relative volatilities which result in most of the reaction taking place in the top and middle section of the column (Figure 8) and, given the negligible heat of reaction, leave temperature change only to occur due to the liquid compositions as determined by the separation. Should heat of reaction not be neglected, more significant temperature changes through the reactive stages would be expected, subject to reflux ratio values. The case studies also show similar behaviour in the composition profiles in Figure 7 where the liquid mole fractions of products C and D increase gradually towards the top and bottom of the column, respectively.

System II (Case studies 6-7)

For System II (Case studies 6 and 7), the relative volatility between the products (α_{CD}) remained the same as for System I (α_{CD}=6), but α_{CA} and α_{BD} were reduced (α_{CA}=α_{BD}=1.2) and the relative volatility between the two reactants was increased (α_{AB}=4.15). The relative volatility between components C and D, α_{CD}, is calculated based on the rest of relative volatilities using the expression: α_{CD}= $\alpha_{CA} \cdot \alpha_{AB} \cdot \alpha_{BD}$. For System II, the optimal results indicate the existence of a single, although larger, reactive column due to the large relative volatility between the reactants, as well as the more difficult separation at both column ends between the reactants and the products. It is also interesting to note that the increased TAC of Case study 7 ($k_{f0}=2.1 \cdot 10^6$ (m^3/(kmol·s)) and K_{eq}=81 with corresponding TAC of 2.541 €/kg) comparing to Case study 6 ($k_{f0}=8.41 \cdot 10^6$ (m^3/(kmol·s)) and K_{eq}=81 with corresponding TAC of 2.138 €/kg), mainly stems from the reduced production rate and not from the increased reflux ratio and total number of stages due to the slower kinetics. As reactant A is more volatile for System II, it moves quicker to the top of the column, thus reducing the residence time of the reaction (i.e. amount of component A in liquid phase). As a result, additional liquid holdup is needed and, as the liquid holdup per stage is fixed, more reactive and/or separation stages are therefore required in order to reach sufficient conversion and maintain the highest possible production rate. An alternative would be increasing reflux ratio, however, OPEX is a more significant contributor to the objective function comparing to CAPEX therefore, increasing the number of stages is preferred in terms of optimal TAC, justifying the choice of the optimiser. For both case studies, the optimal solutions additionally include a vapour stream that is removed from a lower point in the column (stage 25 and stage 33 for Case studies 6 and 7, respectively), and is recycled back to the reactive column, still as vapour, at a higher stage (stage 10 and stage 11, respectively). Simulations were performed for those two case studies, where all the optimal design and operational variables were kept the same, however, the vapour pump-around stream was removed from the column in order to investigate its benefits. The overall cost (TAC) for both case studies, which did not include the vapour pump-around stream, was approximately 0.01% higher showing that the difference, although existing, is limited and that the exact benefits of this novel pump-around stream on the performance of reactive distillation columns should be further investigated, as mentioned earlier.

For Case studies 6-7 most of the temperature change takes place at the top and the bottom of the reactive column whilst temperature remains almost stable in the middle of the column. Sharp temperature changes breaks are also observed, which could potentially be used for inferential composition control. Also, due to the reduced α_{BD}, the temperature level at the bottom of the columns decreased (as the boiling point of component B is fixed to 413 K) therefore, the reaction rates were

reduced comparing to System I (Figure 8~~Figure 8~~). Due to the large difference in reactant volatilities (α_{AB} = 4.15), most of the conversion takes place towards the upper end and middle of the column where both reactants are in liquid phase. For both case studies, the mole fractions of products C and D gradually increase towards the column ends (similarly to System I). However, the larger relative volatility between the reactants (α_{AB} = 4.15) shifts the feed stages (and therefore the mole fraction peaks for the reactants) towards the column ends.

System III (Case studies 8-11)

For System III (Case studies 8, 9, 10 and 11), the relative volatility between the lightest components, α_{CA}, and between the reactants, α_{AB}, remains the same as for System I, however, the boiling point ranking is now alternating: $T_C<T_A<T_D<T_B$, i.e. there is a different boiling point order between one reactant (now high-boiler B) and one product (now middle-boiler D). The optimal results in Table 5~~Table 5~~ indicate that additional units are now required to meet product specifications for this more challenging system.

For Case study 8 ($k_{f0}=8.41\cdot10^6$ (m^3/(kmol·s)) and K_{eq}=81 with corresponding TAC of 2.389 €/kg), a pre-reactor is needed before the reactive distillation column to maximise the conversion (87.3% achieved within the pre-reactor, whilst the maximum expected for an infinitely large CSTR would be 90% given that K_{eq}= 81, and close to 100% within the reactive column) in order to avoid the additional cost of two downstream distillation columns (for product purification) and recycle streams due to the low reaction conversion. For Case study 9 ($k_{f0}=2.1\cdot10^6$ (m^3/(kmol·s)) and K_{eq}=81 with corresponding TAC of 2.963 €/kg), this cost cannot be avoided since in addition to the pre-reactor and the reactive distillation column, two distillation columns are needed for further product purification due to the slower kinetics considered in the reactive units ($2.1\cdot10^6$ (m^3/(kmol·s)), which leads to a lower reaction conversion (85.1% conversion is achieved within the pre-reactor, which increases to 96.6% within the reactive column). Since Case study 9 has the most complex design, the optimal flowsheet is presented in

Figure 9~~Figure 9~~. For Case studies 10 ($k_{f0}=8.41\cdot10^6$ (m^3/(kmol·s)) and K_{eq}=0.184 with corresponding TAC of 4.861 €/kg) and 11 ($k_{f0}=1.05\cdot10^6$ (m^3/(kmol·s)) and K_{eq}=0.184 with corresponding TAC of 6.480

€/kg), the chemical equilibrium considered is very low (K_{eq}=0.184), therefore a pre-reactor does no longer improve the process performance as the conversion in the reactor is limited by chemical equilibrium which for these case studies favours the backward reaction, resulting in very low reactant conversion in a standard reactor. In these cases, in addition to a large reactive column (85 and 78 stages for Case study 10 and 11, respectively), two additional columns are needed to meet the product purity specification. It should be noted that for Case studies 9, 10 and 11, a recycle of the bottom product of DC1 and of the bottom product of DC2 back to the reactive column would be sensible to increase process performance and reduce waste. These two streams should mainly include the unreacted feed (A or B, respectively) as component C is removed as a top product of DC1 (using an additional purity specification ($x_{D,C}$ > 0.99) in the optimisation problem to increase its purity) and component D is removed as a top product of DC2. The absence of a recovery specification for product C in DC1 (as it was not the product of interest), however, led to the bottom stream of DC1 not always containing a large amount of A for Case studies 9, 10 and 11 (0.30, 1.77 and 4.98 kmol/hr, respectively, which correspond to 2.4%, 14% and 39.5% of the initial feed A flow rate) since product C was also present therefore, this additional constraint should be imposed, should this stream is to be considered for recycle. For DC2, the purity and recovery specifications for product D led to the bottom stream containing mainly reactant B for all three case studies (0.39, 1.91 and 5.01 kmol/hr, respectively, which correspond to 3.1%, 15.2% and 39.8% of the initial feed B flow rate). However, as already mentioned, the inclusion of recycles in the superstructure was not possible due to convergence issues therefore, the potential recycle streams were considered waste streams instead.

For Case studies 8-11, temperature changes mainly at the top of the column (unlike System I) where most of the reaction conversion takes place, after which temperature has smaller changes. This can also be seen in Figure 8~~Figure 8~~ where the reaction rate ratio remains almost constant in the middle of the columns due to the almost constant temperature and compositions. This is due to the challenging volatility ranking (reactant B is less volatile than product D) which leads to the requirement of additional reactive trays to minimise the amount of unreacted reactant B as well as due to the high conversion achieved in the pre-reactor (for Case studies 8 and 9 only). For the challenging case studies of System III, alternative configurations could be considered, such as feeding part of A directly to the bottom of the column (and the rest to the pre-reactor) in order to stimulate reaction at the lower part of the reactive column or operating with excess of reactant A. Such configurations are, however, not considered in the current superstructure but could be investigated further as individual designs.

Formatte

System IV (Case studies 12-13)

For System IV (Case studies 12 and 13), the boiling point order is again $T_C<T_A<T_B<T_D$. The relative volatility between the reactants is the same as for System I (α_{AB}=1.5) but the separation at each ends of the column is now more challenging ($\alpha_{CA}=\alpha_{BD}$=1.2). Case study 12 ($k_{f0}=8.41\cdot10^6$ (m^3/(kmol·s)) and K_{eq}=2.25 with corresponding TAC of 2.390 €/kg) has the same kinetic parameters ($k_{f0}=8.41\cdot10^6$, K_{eq}=2.25) as Case studies 2 and 14 and it can be seen that they have the same design (single reactive distillation column), however, the more difficult the separation task, the more demanding the design and operational parameters (i.e. higher total number of stages, higher reflux ratio), as expected. Similarly, Case study 13 ($k_{f0}=8.41\cdot10^6$ (m^3/(kmol·s)) and K_{eq}=81 with corresponding TAC of 2.210 €/kg) has the same kinetic parameters ($k_{f0}=8.41\cdot10^6$, K_{eq}=81) as Case studies 1, 6 and 8, and it can be seen that the more difficult the separation task (including the boiling point order), the more demanding the design and operational parameters, as expected.

For System IV, similarly to System II and System III, temperature at the bottom of the column is lower compared to System I, due to the relative volatilities. Case studies 12 and 13 have a gradually increasing temperature profile similarly to System I, where feed stages only slightly disrupt the smooth increase. The gradually increasing temperature profile is due to the favourable relative volatilities

which result in most of the reaction taking place in the middle of the column and, given the negligible heat of reaction, leave the temperature change only to happen due to separation. Also, better separation between reactants A and B can be observed. In addition, Case study 12 has lower α_{BD} compare to Case studies 2 and 14 which leads to a lower concentration of the heavy reactant B in the middle of the reactive column.

System V (Case studies 14-15)

For System V, i.e. Case study 14 ($k_{f0}=8.41\cdot10^{6}$ ($m^3/(kmol\cdot s)$) and $K_{eq}=0.184$ with corresponding TAC of 2.390 €/kg) and Case study 15 ($k_{f0}=8.41\cdot10^{6}$ ($m^3/(kmol\cdot s)$) and $K_{eq}=2.25$ with corresponding TAC of 2.150 €/kg), the relative volatility between the reactants is higher than for System I and System IV ($\alpha_{AB}=2.5$), and the separation at the top of the column is more challenging ($\alpha_{CA}=1.2$) than at the bottom ($\alpha_{BD}=2$). Case study 12 and Case study 15 have the same reaction parameters, however, the difference in relative volatilities leads to higher temperatures in the column for Case study 15, and therefore to increased forward reaction rates compared to Case study 12 (shown later in Figure 8~~Figure 8~~), leading to a shorter column (27 stages compared to 42 stages). Case study 14 has the same kinetic parameters ($k_{f0}=8.41\cdot10^{6}$, $K_{eq}=2.25$) as Case studies 2 and 12 and it can be seen that they have the same design (single reactive distillation column), however, the more difficult the separation task, the more demanding the design and operational parameters (i.e. higher total number of stages, higher reflux ratio), as expected.

For Case study 14, temperature increases gradually similarly to System I and IV, however, between stages 9 to 25, the profile remains relatively flat, resulting in a steady chemical driving force through these stages (Figure 8~~Figure 8~~). For the same case study, sharp changes are noticed for the mole fractions of products C and D, due to the very high reflux ratio required (10.66) and the large relative volatility between the two products (α_{CD} = 6). This case study has a very low chemical equilibrium ($K_{eq}=0.184$), and is the chemical equilibrium case that benefits the most from the intensified reactive distillation process since it is possible to overcome the unfavourable chemical equilibrium (Figure 8~~Figure 8~~) and reach a high purity product with a single reactive column. For Case study 15, the profiles are similar to those of Case study 14 since the relative volatilities are the same, however, the change in the mole fractions of products C and D are not as sharp due to the lower reflux ratio. In addition, reactant B has a lower mole fraction in the middle of the column due to the faster consumption of the reactants in the reactive zone (Figure 8~~Figure 8~~).

Further notes

Having discussed in a higher level the temperature and composition profiles in Figure 6~~Figure 6~~ and Figure 7~~Figure 7~~, respectively, and as kinetics are of particular interest due to the intensified nature of reactive distillation processes, a more detailed discussion follows with regards to the chemical driving force for the case studies considered. Overall, from Figure 8~~Figure 8~~, it can be seen that for some case studies which belong to Systems I, II, IV and V (i.e. not case studies 8-11), the chemical driving force shows a peak near the feed stage locations as these are the stages where reactant concentrations are highest. Moreover, for these systems, the driving force is higher at the top of the column and decreases towards the bottom of the column. This is reasonable as concentration of component D at the top of the column is negligible. In addition, for the boiling point ranking considered, the unreacted components A and B are both in the liquid phase mainly at the upper part of the column, due to heat transfer (between hot component A and cold component C) and bottom purity specification and boiling point (for component B). As a result, the unreacted A and B (with a mole fraction of less than 0.04) are removed from the top of the column (as at the bottom there is a

purity specification), shifting the reaction equilibrium to the right. However, for case studies which belong to System III (Case studies 8, 9, 10 and 11) where the boiling point ranking is reverse, the unreacted component B is also in higher concentration (compared to the other case studies) through the middle and lower part of the column leading to a driving force increase below the feed stage locations. As a result, for those case studies, the behaviour of the driving force is reverse, i.e. increasing towards the bottom of the column. Also, the driving force remains almost constant for a large number of stages due to the almost constant temperature through the same stages as shown in Figure 6~~Figure 6~~, and presents a peak at the bottom of the column. This peak is due to the increase in concentration of reactant B as shown in Figure 7~~Figure 7~~, as it is the heaviest component and therefore tends to accumulate at the bottom of the column along with a small amount of component A (i.e. mole fraction lower than 0.004), given their low relative volatility (α_{AB}=1.5).

Formatte

Formatte

5.1.3 Discussion

This section aims to evaluate the impact of the reaction/separation characteristics on the objective function as well as on the optimal design and operational parameters found for all the case studies considered. As an overall comment, it is worth mentioning that no case study indicated an optimal solution including a side-stripper and/or side-reboiler. Nevertheless, it is expected that using a different objective function which includes a different contribution of CAPEX/OPEX to the overall cost and/or modelling the process on a larger scale (as it was explained in Section 5.1.1) would potentially indicate the requirement of such units. For instance, if CAPEX contributes more significantly to the overall objective function, a side-reboiler could replace the requirement of a very large reactive column, given a fast reaction and a challenging separation task. In addition, the consideration of different systems, where the remixing effect is observed or thermal coupling is considered, could for instance indicate the requirement of a side-stripper in the optimal process.

Case studies 2 and 6 resulted in a similar optimal value of the objective function (TAC=2.140 and 2.138 €/kg, respectively) although their separation and reaction characteristics are different. This indicates that a system with slower kinetics in combination with an easy separation task (Case study 2) is economically similar to a system with faster kinetics in combination with a relatively more difficult separation task (Case study 6). A qualitative example for this comparison would be the esterification of acetic acid towards amyl acetate (similar to Case study 2) and towards n-butyl acetate (similar to Case study 6). The former reaction scheme has slower kinetics but easier separation task (as in Case study 2) whilst the latter has faster kinetics but a relatively more difficult separation task (as in Case study 6). It is interesting to note that Case studies 1 and 8 had the same kinetics (k_{f0}=8.41·10^6 (m^3/(kmol·s)) and K_{eq}=81), however, the existence of different boiling point rankings had a significant impact on the optimal process design and operation. As mentioned earlier, reverse boiling point rankings (α_{BD}=0.75 for Case study 8) led to lower column temperatures (shown in Figure 6~~Figure 6~~) and therefore reduced forward reaction rates (shown in Figure 8~~Figure 8~~), as the boiling point of component B was fixed. As a result, Case study 8 required a pre-reactor in addition to the reactive column, as well as a higher reflux ratio (6.99 for Case study 8 versus 2.59 for Case study 1) with associated TAC of 2.073 €/kg for Case study 1 compared to 2.389 €/kg for Case study 8. The same applies for Case studies 4 and 11 where for the same kinetics (k_{f0}=1.05·10^6 (m^3/(kmol·s)) and K_{eq}=0.184), reverse boiling rankings (Case study 11) required two additional columns as well as a larger reactive column (78 stages for Case study 11 and 32 stages for Case study 4) and higher reflux ratio for the reactive column (18.24 versus 7.97). Similarly, for Case studies 14 and 10 where the same kinetics (k_{f0}=8.41·10^6 (m^3/(kmol·s)) and K_{eq}=0.184) were considered, different boiling point rankings again resulted in different process design and operational characteristics. Reverse boiling point rankings (Case study 10) required two additional distillation columns as well as a larger reactive column (85 stages for Case study 10 versus 36 stages for Case study 14) as well as a high reflux ratio (36.72 for Case study 10 versus 10.66 for Case study 14). Similarly, for Case studies 1 and 2, the same relative volatilities led to a similar process based on a single reactive column, indicating that different

Formatte

Formatte

reaction kinetics had a limited impact. This is reasonable since for a small relative volatility between the reactants (α_{AB}=1.5), the reactants tend to remain between the feed stage locations and therefore the system can tolerate lower reaction rates (i.e. even for Case study 2 with slower kinetics).

Case studies 1 and 6 also had the same reaction kinetics ($k_{f0}=8.41\cdot10^6$ (m^3/(kmol·s)) and K_{eq}=81), resulting in a simple design for both processes. However, the difference in relative volatilities, with a high relative volatility between the reactants (α_{AB} = 4.15 versus α_{AB} = 1.5) and a lower relative volatility between the top and bottom separations ($\alpha_{CA}=\alpha_{BD}$=1.2 versus $\alpha_{CA}=\alpha_{BD}$=2) for Case study 6, led to the latter being benefited by the vapour pump-around stream for this case study. For Case studies 12 and 14, the TAC obtained is very similar as mentioned earlier, indicating that given fast kinetics, small chemical equilibrium and favourable relative volatilities (Case study 14) are economically equivalent to larger chemical equilibrium with less favourable relative volatilities (Case study 12). Furthermore, for Case studies 8 and 9, when the same relative volatilities were considered (α_{CA}=2, α_{AB}=1.5, α_{BD}=0.75) and chemical equilibrium was high enough to favour the forward reaction (K_{eq}=81), slower kinetics required two additional columns (Case study 9), in addition to the pre-reactor (Case study 8) to meet the specifications. However, when unfavourable chemical equilibrium (K_{eq}=0.184) was considered (Case studies 10 and 11), although the additional columns were still required, the pre-reactor was no longer required since the low chemical equilibrium (K_{eq}=0.184) would favour the backward reaction, therefore not leading to a high reaction conversion. For those two case studies, the slower kinetics (Case study 11) led to a higher cost (TAC=6.480 €/kg versus TAC=4.861 €/kg), which was mainly due to the lower production (bottoms) rate (B_R=7.3 kmol/hr versus B_R=10.6 kmol/hr). Case studies 1 and 13 had the same kinetics ($k_{f0}=8.41\cdot10^6$ (m^3/(kmol·s)) and K_{eq}=81), however, the more challenging separation at both column ends for Case study 13 ($\alpha_{CA}=\alpha_{BD}$=1.2 for Case study 13 instead of $\alpha_{CA}=\alpha_{BD}$=2 for Case study 1) led to a more demanding design in terms of total number of stages and reflux ratio. Finally, Case studies 14 and 15 had the same relative volatilities but different chemical equilibrium, with both requiring a single reactive distillation column. However, as expected, the case study with the lowest chemical equilibrium (Case study 14, K_{eq} = 0.184) led to a more expensive process (TAC=2.390 €/kg versus TAC=2.150 €/kg), both in terms of design (36 versus 27 stages) and operation (reflux ratio of 10.66 versus 3.70).

Overall, it appears that, for the relative volatility and reaction kinetics combinations considered in this work, favourable relative volatilities have more of an impact on the optimal TAC than does favourable kinetics. This can be seen in Figure 10~~Figure 10~~, where the optimal results are visualised as a function of the relative volatility between components B and D (α_{BD}) as this ratio had a significant impact on the process design; the forward pre-exponential factor (k_{f0}) and the chemical equilibrium (K_{eq}). Instead of K_{eq}, for which values 0.184 and 2.25 would be very close and therefore could not be easily distinguished, to enhance clarity in the plot, the equivalent equilibrium conversion (see note 6) was plotted as the z-axis. This map can be used as a guideline for the optimal design of reactive distillation processes when other relative volatility and/or kinetics combinations than the ones presented here are considered. From Figure 10~~Figure 10~~, and the results shown in Table 5~~Table 5~~ and Table 6~~Table 6~~, the following conclusions can be drawn which confirm the anticipated behaviour (from an engineering perspective) for the systems and specifications (e.g. quality constraints, objective function etc.) considered:

1. When reactants are middle-boilers ($\alpha_C<\alpha_A<\alpha_B<\alpha_D$), a single reactive distillation column (with simple or more demanding design in terms of number of stages and/or operation in terms of reflux ratio) is economically favourable.
2. Since the previous point applies to a range of different reaction kinetics (i.e. forward pre-exponential factor and chemical equilibrium values), it appears that relative volatilities (when favourable, in terms of boiling point rankings) have a more significant impact on the optimal design and the cost than does the reaction kinetics.

Formatte
Formatte
Formatte
Formatte

3. For favourable boiling point rankings, when relative volatility between the two reactants (α_{AB}) is large, a vapour pump-around stream may be beneficial in terms of optimal cost and production rate.
4. When reverse boiling point rankings and large value of chemical equilibrium are considered, a pre-reactor is needed. Depending on how slow the kinetics are, additional distillation columns may also be required in order to retrieve the desired product. When chemical equilibrium is low enough to favour the backward reaction, the pre-reactor is no longer favourable, however, additional columns are required to meet the product purity specifications.
5. Reverse boiling point ranking in terms of relative volatility between B and D was found to be critical for the design of the process since the main desired product was D. Similarly, if the main desired product was component C, the relative volatility which would be critical would consequently be between C and A, and ancillary equipment is expected to be required when $\alpha_{CA}<1$ (not shown).
6. The value of the reflux ratio when the optimal solution indicates the existence of a single reactive column, depends greatly on the chemical equilibrium of the reaction. Consider fast kinetics and large α_{BD} ($\alpha_{BD}=2$) for instance. For $K_{eq}=81$, a low reflux ratio is required (2.59 – Case study 1), however, for $K_{eq}=2.25$, a higher reflux ratio is needed (3.70 – Case study 15), and for $K_{eq}=0.184$, a very high reflux ratio (10.66 – Case study 14) is needed. A similar argument can be made for the need for increasing number of stages (18, then 27 and then 36, respectively). Similarly, consider slow kinetics and the same large α_{BD} ($\alpha_{BD}=2$) for instance. For $K_{eq}=2.25$, a lower reflux ratio is required (5.76 – Case study 3), however, for $K_{eq}=0.184$, a higher reflux ratio (7.97 – Case study 4) is needed.

These results, in terms of the units included in the optimal process flowsheet, were considered in relation to the reactive distillation feasibility framework presented by Kiss (2013). Although his framework is based on a number of preliminary data (e.g. VLE, reaction kinetics etc.), and not on rigorous optimisation as performed in this work, the overall suggestions in terms of process feasibility and design show very good agreement between his shortcut method and our optimisations.

5.2 Impact of liquid holdup

Liquid holdup is one of the most important parameters for reactive distillation systems, not only determining column pressure drop and hydraulics (e.g. tray weir height) as in conventional distillation, but for reactive distillation also providing the required residence time for the liquid-phase reaction to take place. Large liquid holdup leads to increased weir height and column pressure drop, whilst small liquid holdup may lead to incomplete reaction conversion. The value of the liquid holdup is therefore a very important process parameter in reactive distillation since it is directly linked to the chemical conversion.

In this section, the impact of liquid holdup (h) on the optimal design is investigated. Case study 1 and Case study 5 were selected for the investigation in order to consider the impact of both fast and slower kinetics, for the same separation and chemical equilibrium parameters. Optimisation was performed using the input given in Table 2~~Table 2~~ to Table 4~~Table 4~~ for a number of different liquid holdups ranging from 0.05 m^3/tray to 0.12 m^3/tray (note that so far, the liquid holdup has been assumed constant at 0.1 m^3/tray, and not considered a decision variable due to software limitations). The authors are aware that further increase of the value of liquid holdup beyond 0.12 m^3/tray would potentially be beneficial for the process, however, it is expected that there would be an upper limit on the value of liquid holdup due to increased weir heights and larger column pressure drop, however, this has not been considered in this work. All other parameters were kept the same for all optimisations, as the aim of this section is solely to investigate how the optimal design depends on the liquid holdup.

The optimal designs are found for a number of different liquid holdup values (

Table 7~~Table 7~~ and Figure 11~~Figure 11~~).
From

Table 7~~Table 7~~ it can be seen how the optimal results change based on the liquid holdup considered for both Case study 1 (Table 7a) and Case study 5 (Table 7b). As holdup increases, TAC decreases although only marginally for Case study 1 (approximately 0.1%). This is because as liquid holdup increases, the requirements for total number of stages and reflux ratio decrease. These differences are more visible for Case study 5 (TAC reduced by 0.7%) where kinetics are slower and therefore the system is more sensitive to changes in reaction volume (i.e. liquid holdup). This shows that dedicated reactive distillation internals, that can hold high liquid volumes, might be very promising for relative slow equilibrium limited reactions as they can further reduce the overall cost. For Case study 5 and for holdups lower than 0.07 m^3/tray, the optimal designs have lower reflux ratio than the expected and this is because from an economic point of view, it was more beneficial to reduce production rate (and thereby increase TAC) than to increase the reflux ratio by a large amount in order to maintain production at the same value (12.6 kmol/hr). Note that, if tray weir height had been considered in the objective funtion (currently it is not), then more significant differences would be observed as the holdup (and therefore weir height) increased. Feed stage location and bottom flow rate were found to be almost constant for all designs for Case study 1 due to the fast kinetics which could tolerate the reduction in liquid holdup. For Case study 5, however, feed stage location for the bottom feed varied proportionally with the liquid holdup, due to the slower kinetics present. It is therefore expected that differences in the optimal designs for different holdups will be more significant as kinetics become more challenging.

The most demanding design is the design for the lowest holdup of 0.05 m^3 per (reactive) tray considered for both case studies, which is expected as the residence time for the reaction is then the lowest. If the optimal design found for the lowest holdup of 0.05 m^3/tray (RR_R, B_R, N_{FR1}, N_{FR2}, N_{TR}) was considered for a process with an actual holdup of 0.1 m^3/tray, then the additional stages (20-18=2 stages for case study 1 and 37-29=8 stages for case study 5) beyond the initial requirement will tolerate slower (than the assumed) reaction rates and will enhance reaction and separation without increasing the TAC beyond that of the 0.05 m^3/tray optimal design, and the reflux ratio could decrease slightly without violating the product specifications. In other words, by using the most demanding holdup case (0.05 m^3/tray) as a design basis, a more flexible design is achieved which is suitable for slower kinetics without greatly affecting the TAC. Where there is uncertainty in the reaction kinetics, this may therefore be a design strategy to ensure a flexible and robust design.

Figure 11~~Figure 11~~a and Figure 11~~Figure 11~~b show how TAC, CAPEX and OPEX, changes for the different holdup cases, for Case study 1 and Case study 5, respectively. As presented in

Table 7~~Table 7~~a and

Table 7~~Table 7~~b, an increase in liquid holdup reduces TAC slightly, including OPEX and CAPEX individually, and more so for slower reactions. This is due to the fact that larger holdup leads to higher conversion, which in turn demands less reflux and fewer reactive stages for the same production rate, which is not generally the case for separation only. (Note that the CAPEX results are not smooth as the number of stages is an integer decision.)

5.3 Impact of total number of stages

In Section 5.2 and for Case study 1 and Case study 5, it was found that different holdups lead to different optimal designs, but that those designs, in terms of total number of stages and feed stage locations, did not have a significant impact on the value of the TAC. This section will consider adding a small number of stages to the optimal design (N_{TR}=18) to demonstrate that adding a few additional stages could potentially mitigate production failure issues (i.e. not meeting the process specifications) with a slight, almost negligible, increase in total processing cost. For the optimal design of Case study 1 (reactive distillation only), one stage at a time was added (feed stage locations were moved accordingly for consistency) and the associated TAC was recorded (Figure 12~~Figure 12~~). The rest of the input parameters remained the same, so that CAPEX would be the main contributor to the change in the objective function. Removing one stage at a time, to consider the opposite situation, would require the adjustment of operational parameters (i.e. increase of RR) in order to meet specifications. As a result, straight comparisons would not be possible as both CAPEX and OPEX would be affected so this case was not considered.

Formatte

From Figure 12~~Figure 12~~a it can be seen that increasing the total number of stages has only a small impact on the objective function. This finding supports the idea of a flexible design since adding a few stages in the column will not increase the cost of the investment by much, and at the same time will ensure that there are additional separation and reactive stages in case of a disturbance, thus mitigating a production failure issue.

Formatte

Figure 12b shows the dependence of OPEX and CAPEX separately as a function of the total number of stages. Increasing the total number of stages with increments of 1 leads to an increase of both CAPEX and OPEX with CAPEX increasing significantly as more stages lead to a higher shell and internals cost. OPEX, on the other hand, is only marginally increasing. As the rest of the operational costs (i.e. feed cost, reboiler duty and waste) remain almost constant, this increase is mainly due to a higher maintenance value, as maintenance is a function of CAPEX as described in Appendix A2.

6. Conclusions

In this work, a novel methodology has been presented for the simultaneous optimisation of the design and operation of a complex reactive distillation process. Based on a superstructure approach, various process alternatives were considered. gPROMS ProcessBuilder was used to solve the MINLP problem and to find the optimal design and operating parameters of the process for a number of industrially relevant case studies varying in the key system characteristics (i.e. reaction kinetics and separation parameters). Although generic case studies were considered in order to allow comparisons between the cases, the methodology can just as easily be applied to real systems of industrial relevance, with or without the underlying assumptions of the cases considered in this work.

The requirement of a single reactive distillation column for systems with favourable relative volatilities demonstrated that reactive distillation is an economically attractive Process Intensification (PI) example, compared to the conventional process of a reactor followed by two regular distillation columns. For systems with more challenging relative volatilities, e.g. the product is a middle-boiler, it was found that a pre-reactor, and even two additional columns for further purification, may be required depending on the reaction kinetics, demonstrating that the methodology can be applied also in such challenging cases.

Overall, it was shown that the system characteristics do impact on the optimal design and operation, and that the extent of the impact depends on the relative contributions from separation performance and from kinetics. A 3-D figure representing the optimal results was presented that illustrates the relative contributions of key parameters to the optimal design, in particular, in relation to the number of units required.

Future work will focus on expanding the methodology to include recycle streams which currently could not be investigated due to the mathematical complexity of the problem and challenging initialisation procedures and on including more optimisation variables, such as column pressure profiles due to its impact on both reaction and separation performance.

7. References

Alcántara-Avila, R., Sillas-Delgado, H. A., Segovia-Hernández, J. G., Gómez-Castro, F. I. and Cervantes-Jauregui, J.A. (2015). "Optimization of a reactive distillation process with intermediate condensers for silane production." Computers and Chemical Engineering 78: 85-93.

Almeida-Rivera, C. P., Swinkels, P. L. J. and Grievink, J. (2004). "Designing reactive distillation processes: present and future." Computers & Chemical Engineering **28**(10): 1997-2020.

Barbosa, D. and Doherty, M. F. (1988). "The simple distillation of homogeneous reactive mixtures." Chemical Engineering Science **43**(3): 541-550.

Biegler, L. T. (2010). Nonlinear Programming: Concepts, Algorithms, and Applications to Chemical Processes, Society for Industrial and Applied Mathematics.

Bisowarno, B. H., Tian, Y. C. and Tadé, M. O. (2004). "Application of side reactors on ETBE reactive distillation." Chemical Engineering Journal **99**(1): 35-43.

Boodhoo, K. and Harvey, A. (2013). Process Intensification: An Overview of Principles and Practice. Process Intensification for Green Chemistry, John Wiley & Sons, Ltd**:** 1-31.

Buzad, G. and Doherty, M. F. (1994). "Design of three-component kinetically controlled reactive distillation columns using fixed-points methods." Chemical Engineering Science **49**(12): 1947-1963.

Buzad, G. and Doherty, M. F. (1995). "New tools for the design of kinetically controlled reactive distillation columns for ternary mixtures." Computers & Chemical Engineering **19**(4): 395-408.

Cardoso, M. F., Salcedo, R. L., de Azevedo, S. F. and Barbosa, D. (2000). "Optimization of reactive distillation processes with simulated annealing." Chemical Engineering Science **55**(21): 5059-5078.

Ciric, A. R. and Gu, D. (1994). "Synthesis of nonequilibrium reactive distillation processes by MINLP optimization." AIChE Journal **40**(9): 1479-1487.

Frey, T. and Stichlmair, J. (2000). MINLP optimization of reactive distillation columns. Computer Aided Chemical Engineering. S. Pierucci, Elsevier. **8:** 115-120.

Georgiadis, M. C., Schenk, M., Pistikopoulos, E. N. and Gani, R. (2002). "The interactions of design control and operability in reactive distillation systems." Computers & Chemical Engineering **26**(4): 735-746.

Halvorsen, I. and Skogestad, S. (2000). "Distillation Theory." Encyclopedia of Separation Science.

Harmsen, G. J. (2007). "Reactive distillation: The front-runner of industrial process intensification: A full review of commercial applications, research, scale-up, design and operation." Chemical Engineering and Processing: Process Intensification **46**(9): 774-780.

Huang, K., Iwakabe, K., Nakaiwa, M. and Tsutsumi, A. (2005). "Towards further internal heat integration in design of reactive distillation columns—part I: The design principle." Chemical Engineering Science **60**(17): 4901-4914.

Infochem/KBC Advanced Technologies plc (2019), Multiflash, https://www.kbc.global/software/advanced-thermodynamics/

Ismail, S. R., Proios, P. and Pistikopoulos, E. N. (2001). "Modular synthesis framework for combined separation/reaction systems." AIChE Journal **47**(3): 629-649.

Jackson, J. R. and Grossmann, I. E. (2001). "A disjunctive programming approach for the optimal design of reactive distillation columns." Computers & Chemical Engineering **25**(11–12): 1661-1673.

Kiss, A. A. (2013). Reactive Distillation. Advanced Distillation Technologies, John Wiley & Sons, Ltd**:** 353-392.

Lee, J. W., Hauan, S. and Westerberg, A. W. (2000). "Graphical methods for reaction distribution in a reactive distillation column." AIChE Journal **46**(6): 1218-1233.

Lee, J. W. and Westerberg, A. W. (2000). "Visualization of stage calculations in ternary reacting mixtures." Computers & Chemical Engineering **24**(2): 639-644.

Lee, J. W. and Westerberg, A. W. (2001). "Graphical design applied to MTBE and methyl acetate reactive distillation processes." AIChE Journal **47**(6): 1333-1345.

Lee, H. Y., Lai, I. K., Huang, H. P. and Chien, I. L. (2012). "Design and Control of Thermally Coupled Reactive Distillation for the Production of Isopropyl Acetate." Industrial & Engineering Chemistry Research **51**(36): 11753-11763.

Lima, R. M., Salcedo, R. L. and Barbosa, D. (2006). "SIMOP: Efficient reactive distillation optimization using stochastic optimizers." Chemical Engineering Science **61**(5): 1718-1739.

Luyben, W. L. and Yu, C.C. (2008). Reactive Distillation Design and Control, John Wiley & Sons, Inc.

Ma, Y., Luo, Y. and Yuan, X. (2019). "Equation-oriented optimization of reactive distillation systems using pseudo-transient models." Chemical Engineering Science **195**: 381-398.

Mahajani, S. M. and Kolah, A. K. (1996). "Some Design Aspects of Reactive Distillation Columns (RDC)." Industrial & Engineering Chemistry Research **35**(12): 4587-4596.

Nguyen, N. and Demirel, Y. (2011). "Using thermally coupled reactive distillation columns in biodiesel production." Energy **36**(8): 4838-4847.

Panjwani, P., Schenk, M., Georgiadis, M. C. and Pistikopoulos, E. N. (2005). "Optimal design and control of a reactive distillation system." Engineering Optimization **37**(7): 733-753.

Papalexandri, K. P. and Pistikopoulos, E. N. (1996). "Generalized modular representation framework for process synthesis." AIChE Journal **42**(4): 1010-1032.

Reepmeyer, F., Repke, J. U. and Wozny, G. (2004). "Time optimal start-up strategies for reactive distillation columns." Chemical Engineering Science **59**(20): 4339-4347.

Process Systems Enterprise (2020). gPROMS, https://www.psenterprise.com/products/gproms/processbuilder, 1997-2020.

Sargent, R. W. H. and Gaminibandara, K. (1976). Optimum Design of Plate Distillation Columns. Optimization in Action;. London, Academic Press.

Seferlis, P. and Grievink, J. (2001). "Optimal Design and Sensitivity Analysis of Reactive Distillation Units Using Collocation Models." Industrial & Engineering Chemistry Research **40**(7): 1673-1685.

Smith, E. M. (1996). "On the Optimal Design of Continuous Processes". PhD. Dissertation under supervision of Pantelides, C., Imperial College of Science, Technology and Medicine, London U.K.

Subawalla, H. and Fair, J. R. (1999). "Design Guidelines for Solid-Catalyzed Reactive Distillation Systems." Industrial & Engineering Chemistry Research **38**(10): 3696-3709.

Tang, Y. T., Chen, Y. W., Huang, H. P., Yu, C. C., Hung, S. B. and Lee, M. J. (2005). "Design of reactive distillations for acetic acid esterification." AIChE Journal **51**(6): 1683-1699.

Tian, Y., Pappas, I., Burnak, B., Katz, J. and Pistikopoulos, E.N. (2020). "A Systematic Framework for the synthesis of operable process intensification systems – Reactive separation systems." Computers & Chemical Engineering **134**: 106675.

Tung, S. T. and Yu, C. C. (2007). "Effects of relative volatility ranking to the design of reactive distillation." AIChE Journal **53**(5): 1278-1297.

Urselmann, M., Barkmann, S., Sand, G. and Engell, S. (2011). "Optimization-based design of reactive distillation columns using a memetic algorithm." Computers & Chemical Engineering **35**(5): 787-805.

Viswanathan, J. and Grossmann, I. E. (1990). "A combined penalty function and outer-approximation method for MINLP optimization." Computers & Chemical Engineering **14**(7): 769-782.

Vora, N. and Daoutidis, P. (2001). "Dynamics and Control of an Ethyl Acetate Reactive Distillation Column." Industrial & Engineering Chemistry Research **40**(3): 833-849.

Wang, S. J., Lee, H. Y., Ho, J. H., Yu, C. C., Huang, H. P. and Lee, M. J. (2010). "Plantwide Design of Ideal Reactive Distillation Processes with Thermal Coupling." Industrial & Engineering Chemistry Research **49**(7): 3262-3274.

Wang, S. J., Wong, D. S. H. and Yu, S. W. (2008). "Design and control of transesterification reactive distillation with thermal coupling." Computers & Chemical Engineering **32**(12): 3030-3037.

Yeomans, H. and Grossmann, I. E. (1999). "A systematic modeling framework of superstructure optimization in process synthesis." Computers & Chemical Engineering **23**(6): 709-731.

Appendix A1

This Appendix outlines how the chemical components considered in this work were modelled in Multiflash v6.1 (Infochem 2019) in order to obtain the desired boiling point (volatility) rankings. Multiflash is a software where chemical components and their properties are modelled and the file created is then imported by ProcessBuilder in order to use these components and their properties in the process flowsheet.

Vapour pressure (in Pa) in Multiflash is calculated using the following Antoine equation:

$$ln\ P_i = A_i + \frac{B_i}{T+C_i} + D_i T^{F_i} + E_i lnT + \frac{G_i}{T^2}\ \ for\ T_{min} \leq T \leq T_{max} \quad \text{(A1.1)}$$

If the 3rd term onwards is not used, then D_i=0, F_i=1 and E_i=G_i=0. In this work, differences in the dependence of vapour pressure on temperature between components are ignored, therefore all the Antoine coefficients except A_i were considered *equal* for all components *i*.

As a result, for two components *i=a, b*, their vapour pressures are related as follows:

$$ln\ P_a - ln\ P_b = A_a\ - A_b \quad \text{(A1.2)}$$

The relative volatility α_{ab} can be expressed based on relative vapour pressures using the following relationship:

$$ln(P_a/P_b) = ln(\alpha_{ab}) = A_a - A_b \quad \text{(A1.3)}$$

For instance, let's consider a desired relative volatility of α_{ab} = 2:

$\ln(2) = 0.693 = \mathrm{A}_a - \mathrm{A}_b$ so if for instance $A_a = 10$ then A_b must be 9.307.

As mentioned above, the Antoine coefficients B_i, C_i, D_i, E_i, F_i and G_i are considered equal for all components *i*, using the values of the reference component, which is in this work is for the heavy reactant, component B, for all case studies as shown in Table A1.

Appendix A2

Although ProcessBuilder, which is the tool used for simulation and optimisation in this work, provides functionalities for economic evaluation, it was decided to nevertheless use open source costing functions such that a more comprehensive analysis of different costing elements could be considered. The objective function considered is taken to be the production-based total annualised cost of the process (in €/ktn), which is the sum of annualised capital and operating costs (in €/yr) divided by the annual production rate (in ktn/yr):

Production-based TAC (€/ktn) = TAC (€/yr) / Production rate (ktn/yr)

The main reference considered for the costing functions is Coulson and Richardson's textbook (Sinnott and Towler 2020) although other textbooks (e.g. Seider et al. 2009) could also be used for comparison.

Total Annualised Cost, *TAC*, is the sum of the annualised capital cost, *annual. CAPEX,* and the annualised operating cost, *annual. OPEX*:

TAC (€/yr) = annual. CAPEX + annual. OPEX

Capital cost includes the bare equipment cost of all the units considered and is multiplied by a Lang factor to also include the installation cost. Note that the correlations used to calculate the CAPEX does not include cost of land, control room or feedstock/product storage. Cost indices are used to bring the costs up to present costs (January 2019). Furthermore, interest rate and depreciation of the capital cost are also considered.

Operating cost includes feedstock, utilities and waste treatment costs, as well as maintenance costs, and are based on 2019 costs, hence cost indices are not needed.

Both capital and operating costs need to be annualised (i.e. expressed as cost per year of plant operation) so that the total annualised cost, *TAC*, can be used as a profitability measure for the comparison of various process alternatives.

In Table B1 and Table B2, mathematical expressions for capital (Table B1) and operating (Table B2) costs are presented, followed by a description of how these are annualised.

A) Capital Cost Estimation

In Table B1, the equations used to calculate the individual equipment costs are listed, which are based on the cost correlations suggested by Coulson and Richardson (Sinnott and Towler 2020). All the cost variables within these correlations (also called driver-cost variables, e.g. W_{shell} in the C_{DC} calculation) were taken from gPROMS ProcessBuilder to ensure consistency. For instance, the distillation column shell weight in gPROMS ProcessBuilder is calculated based on column diameter, shell thickness, material density and column length as explained by Seider et al. (Seider et al. 2009). In addition, valves are not included in Table B1 as valve cost is typically included in installation cost (see Lang factor below). With regards to distillation column cost, Carpenter 20CB-3 was assumed as column shell and column internals' material to increase corrosion resistance. Therefore, as the correlation of C_{DC} was based on 304 stainless steel, the latter was then multiplied by 1.9, to take into consideration the specific material cost (Seider et al. 2009).

The value of the heat transfer coefficient (750 $W/m^2 \cdot K$) for the calculation of the condenser and reboiler duty (see Note 7) was chosen using an average value for a tubular reboiler with evaporation with natural circulation and for a tubular condenser (Engineering ToolBox 2003). For both units, a temperature difference of 10 K was assumed as this is a reasonable value for the heating and cooling medium temperature difference in condensers and reboilers of distillation columns (Engineering Toolbox 2004). For the reflux drum capacity calculation, a residence time of 5 min was assumed (Seider

et al. 2009). The dollar exchange rate was taken as 0.9 €/$ based on the average value for the rates published between January 2019 and January 2020 (Reuters 2020). Finally, interest rate (15%), plant life (10 years) and annual operating hours (8000 hrs/yr) were considered reasonable values from an industrial point of view, which were in agreement with the ranges provided by Coulson and Richardson (Sinnott and Towler 2020).

The bare equipment cost is then given by:

$$C_{T1}(\$) = N_{DC}\cdot C_{DC} + N_{ST}\cdot C_{ST} + N_R\cdot C_R + N_C\cdot C_C + N_S\cdot C_S + N_{RC}\cdot C_{RC} + N_{RD}\cdot C_{RD} \quad \text{(A2.1)}$$

where N_i is the total number of units *i* of each type of equipment used, i.e. *i = [DC, ST, R, C, S, RC, RD]*

In equation A2.1 and as shown in the notation list, DC stands for distillation column, ST for sieve trays, R for reboiler, C for condenser, S for stripper, RC for reactor and RD for reflux drum. To account for installation cost, bare equipment cost is usually multiplied by a Lang factor (a_{Lang}) in order to provide an estimate of the fixed capital cost. For a processing plant predominantly handling fluids, the Lang factor, a_{Lang}, is usually assumed to be 4 (Sinnott and Towler 2020). Taking into consideration conversion from dollars to euros ($rate_{exch}$, assumed to be equal to 0.9 €/$), the fixed capital cost is finally expressed as:

$$CAPEX_1(€) = 4 \cdot C_{T1} \cdot 0.9(€/\$) = 3.6 \cdot C_{T1} \quad \text{(A2.2)}$$

B) Operating Costs Estimation

Table B2 presents the equations used for the calculation of each type of operational cost, based on utility costs provided by Nouryon. The cost of cooling water for the condenser is ignored. Although feed cost is much larger than the other operating costs, leading to OPEX being much larger than CAPEX, it was nevertheless included in the objective function due to its significance as a cost factor. In more detail, the objective function was defined as the overall cost (capital and operating) divided by the production rate in order to minimise the overall cost to the lowest possible per amount of the desired component produced (i.e. minimise costs whilst maximising production rate). Therefore, feed cost was included so that the objective function would take into account design and energy costs, considering the cost related to incomplete reactant conversion (i.e. product losses) and/or product recovery for the given fixed feed flow rate since production rate was not fixed.

With regards to the operational cost related to waste treatment, further treatment is needed for streams that contain aqueous products with organic impurities. In the case studies presented in this work, component C was considered to be aqueous whilst components A, B and D were considered to be organic compounds, based on esterification systems often appearing in literature (e.g. Luyben and Yu 2008). As a result, waste treatment for all case studies was calculated for the streams that contained mainly product C (e.g. distillate stream from reactive distillation column for Case study 1 etc.) with some organic impurities i.e. component A, B and/or D. If this stream did not contain any organic impurities (e.g. in case of a single reactive column and full reactant conversion) then waste treatment cost was calculated as zero.

The total (not annualised) operation cost is the sum of all the individual operating costs:

$$OPEX\ (€/s) = C_{OS} + C_{OF} + C_{OW} + C_{main} \quad \text{(A2.3)}$$

C) Annualisation of the costs

As explained earlier, annualisation is necessary so that the total annualised cost, TAC, can be used for the direct comparison of profitability of various process alternatives. However, before annualisation,

the equipment cost, which was based on 2007 prices (Sinnott and Towler 2020), needs to be brought up to present cost and this is done by the use of cost indices.

Two different cost indices, CEPCI (Chemical Engineering Plant Cost Index) and NF (Nelson-Farrar Refinery Construction Cost), were considered by Coulson and Richardson (Sinnott and Towler 2020) to account for price inflation of equipment. CEPCI will be used in this work as it applies to an average of all chemical processing industries whilst NF is restricted to the petroleum industry (Seider et al. 2009).

When updating the cost, equipment cost based on a reference year (2007) is multiplied by the ratio of the current year's index (e.g. 2019, CEPCI = 619.2) to the reference's year index (2007, CEPCI = 509.7). Thus, costs for 2019 are updated as follows:

$$CAPEX_{2019}\,(€) = CAPEX_1 \cdot \left(\frac{CEPCI_{2019}}{CEPCI_{2007}}\right) = CAPEX_1 \cdot \left(\frac{619.2}{509.7}\right) = 1.21 \cdot CAPEX_1 \quad \text{(A2.4)}$$

The 2019 index has been used here based on the preliminary 2019 CEPCI index (Jenkins 2019), as this was the only value available when this work started, but can be updated when more recent index values become publicly available.

For the capital costs, one also needs to take into account investment rate and depreciation. These two cost elements can be taken into account as follows (Sinnott and Towler 2020), assuming that the interest rate is 15% and that the plant life is 10 years as previously stated:

$$CRF\ (yr^{-1}) = \frac{interest}{\left(1-(1+interest)^{-plant\ life}\right)} = \frac{0.15}{\left(1-(1+0.15)^{-10}\right)} = 0.20 \quad \text{(A2.5)}$$

There are other methods for the consideration of interest rate and depreciation based on literature (Seider et al. 2009), however, these methods require more data such as plant salvage value at the end of the plant life. The equation above was therefore chosen based on its simplicity.

The final annualised capital cost, including investment rate and depreciation (CRF), can then be expressed as follows:

$$\textbf{annual. CAPEX}\ (€/yr) = CAPEX_{2019}(€) \cdot CRF\ (1/yr) = CAPEX_{2019}(€) \cdot 0.20\ (1/yr) = 0.20 \cdot CAPEX_{2019} \quad \text{(A2.6)}$$

To annualise the operating cost, assuming 8000 hr/yr operation (to take into consideration yearly shut-down for maintenance during which there is no plant operation), the calculation is as follows:

$$\textbf{annual. OPEX}\ (€/yr) = OPEX\ (€/s) \cdot 8000\ (hr/yr) \cdot 3600\ (s/hr) = 288 \cdot 10^5 \cdot OPEX\ (€/yr) \quad \text{(A2.7)}$$

Total Annualised Cost (TAC) is then the sum of the annualised CAPEX and OPEX, thus calculated as:

$$\textbf{TAC (€/yr) = annual. CAPEX + annual. OPEX} \quad \text{(A2.8)}$$

As a result, the final form of the objective function is as follows:

$$\textbf{Production-based TAC (€/ktn) = TAC (€/yr) / Production rate (ktn/yr)} \quad \text{(A2.9)}$$

Notation list[1]

A	Heat exchange area (m^2)
a_{Lang}	Lang factor (-)
annual. CAPEX	Capital (annualised) cost (€/yr)
annual. OPEX	Operating (annualised) cost (€/yr)
$CAPEX_1$	Capital cost (including purchase and installation) (€)
$CAPEX_{2019}$	Capital cost (incl. purchase and installation) brought up to 2019 (€)
C_C	Condenser purchase cost ($)
C_{DC}	Distillation column purchase cost ($)
CEPCI	Chemical Engineering Plant Cost Index (-)
C_{main}	Plant maintenance operating cost (€/s)
C_{OF}	Feed cost (€/s)
C_{OS}	Steam cost (€/s)
C_{OW}	Waste treatment cost (€/s)
C_R	Reboiler purchase cost ($)
C_{RC}	Reactor purchase cost ($)
C_{RD}	Reflux drum purchase cost ($)
CRF	Interest rate and depreciation factor (1/yr)
C_S	Stripper purchase cost ($)
C_{ST}	Sieve trays purchase cost ($)
C_{T1}	Total purchase cost ($)
D_i	Internal column diameter (in)
D_o	External column diameters (in)
D_{tray}	Tray diameter (m)
d	Density of column construction material (0.284 lb/in^3)
E	Fractional weld efficiency (85%)
F_{OW}	Organic waste flow rate (kg/s)
F_T	Total feed flow rate (kg/s)
L	Tangent-to-tangent column height (in)
N_i	Number of equipment units (-)
OPEX	Total operating cost (€/s)
P_d	Internal design gauge pressure (psig)
$Q_{condenser}$	Condenser heat duty (W)
$Q_{reboiler}$	Reboiler heat duty (W)
$rate_{exch}$	Dollars to euros exchange rate (€/$)
S	Maximum allowable stress (15000 lb_f/in^2)
TAC	Total Annualised Cost (€/yr)
t_p	Internal pressure thickness (in)
t_s	Column head and shell thickness (in)
t_w	Thickness to withstand wind at the bottom (in)
V	Reflux drum capacity (m^3)
V_R	Reactor volume (m^3)
W	Stripper shell weight (kg)
W_{shell}	Column shell weight (kg)

[1] Additional symbols related to the superstructure variables are included in Table 1.

References (Appendices):

Engineering ToolBox (2003). *Heat Exchanger Heat Transfer Coefficients*. Retrieved from: https://www.engineeringtoolbox.com/heat-transfer-coefficients-exchangers-d_450.html [Accessed 28/10/2019].

Engineering ToolBox (2004). *Cooling Tower Efficiency*. Retrieved from: https://www.engineeringtoolbox.com/cooling-tower-efficiency-d_699.html [Accessed 28/10/2019].

Infochem/KBC Advanced Technologies plc (2019), Multiflash, https://www.kbc.global/software/advanced-thermodynamics/ [Accessed 30/09/19].

Jenkins, S. (2019). Chemical Engineering. CEPCI Updates: January 2018 (Prelim.) and December 2017 (Final). Retrieved from: https://www.chemengonline.com/2019-cepci-updates-january-prelim-and-december-2018-final/ [Accessed 30/09/19].

Luyben, W. L. and Yu, C. C. (2008). Reactive Distillation Design and Control, John Wiley & Sons, Inc.

Reuters (2020). Dollars to euros exchange rate. Retrieved from: https://www.reuters.com/finance/currencies/quote?srcCurr=EUR&destCurr=USD [Accessed 30/09/19].

Seider, W. D., Lewin, D. R., Seader, J. D., Widagdo, S., Gani, R., Ng, K. M. (2009). *Product and Process Design Principles: Synthesis, Analysis and Evaluation*. (4th ed.). USA: John Wiley and Sons.

Sinnott, R. K. and Towler, G. (2020). *Coulson & Richardson's chemical engineering*. Vol. 6. (6th ed.). Oxford: Elsevier Butterworth-Heinemann.

Figures and Tables

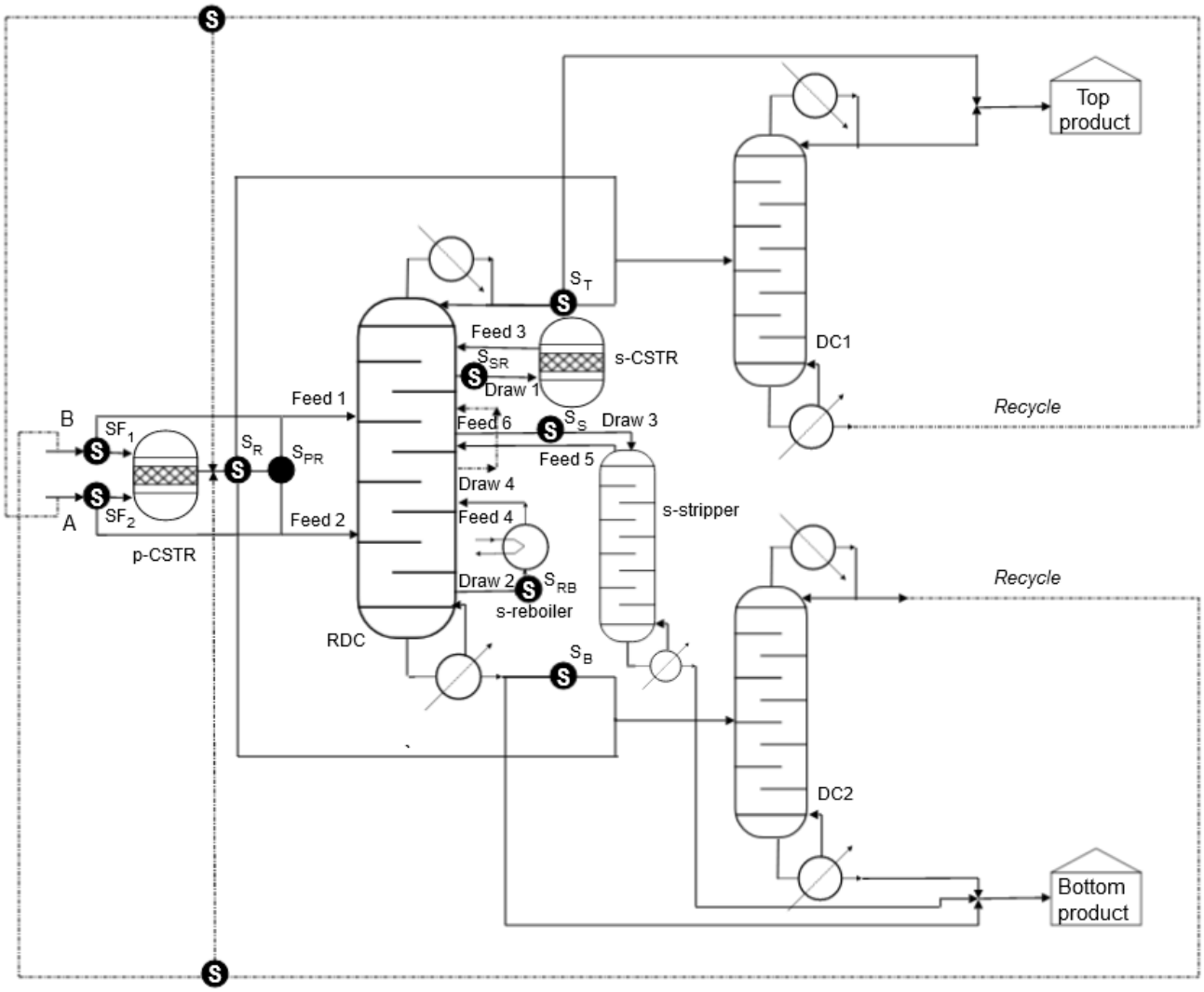

Figure 1: Reactive distillation superstructure (variables shown in Table 1). The black nodes with the ~~red coloured~~symbol *S* show alternative stream directions, indicating units being included or excluded from the optimal process. The black node without the ~~red colored~~symbol *S* shows a potential feed split which is a continuous variable.

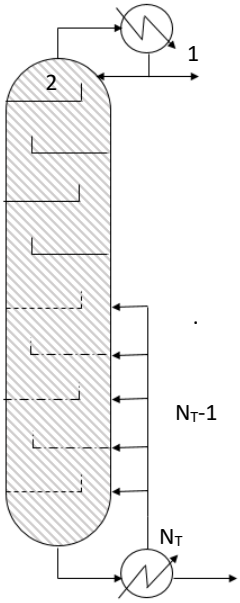

Figure 2: Optimisation of total number of stages in gPROMS ProcessBuilder. Feed streams, side-draw streams and variables related to the reactive distillation column (e.g. reflux ratio) are not shown for clarity.

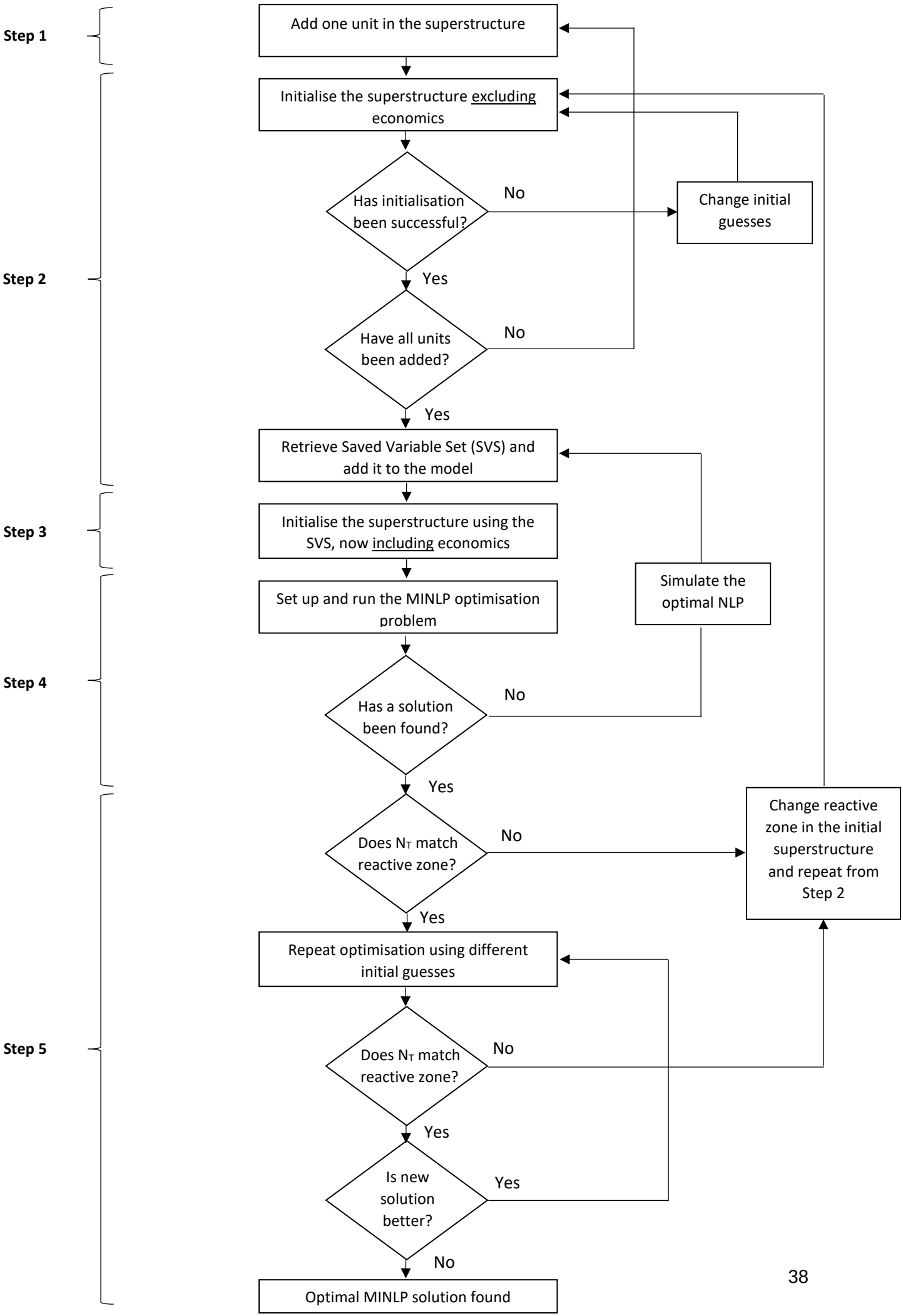

Figure 3: Simultaneous MINLP optimisation strategy as performed in gPROMS ProcessBuilder.

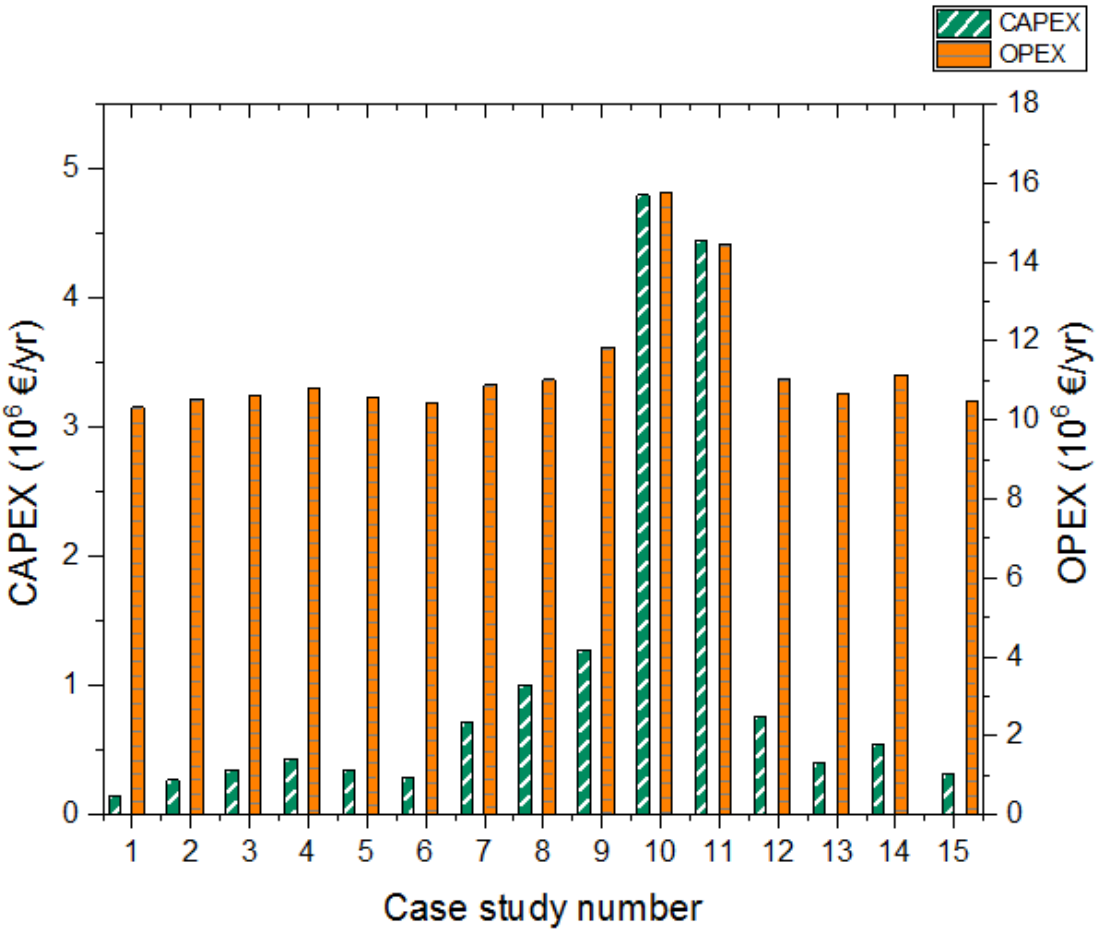

Figure 4: CAPEX and OPEX comparison for the optimal designs considered for all case studies (Table 5).

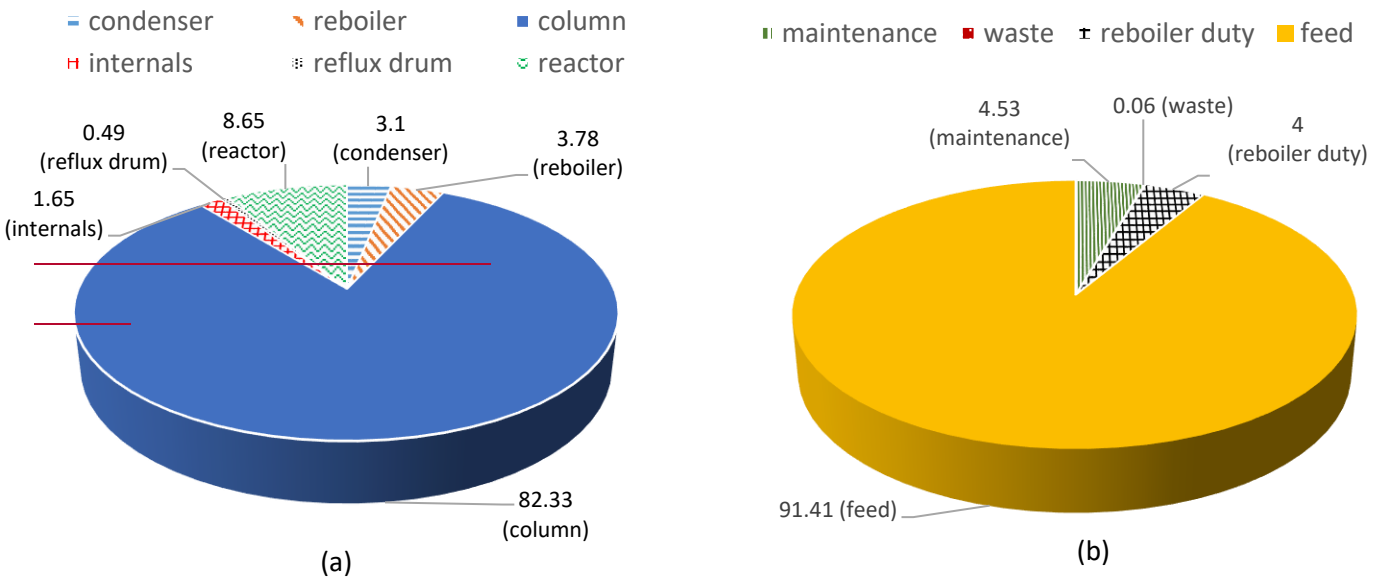

Figure 5: Capital (a) and operating (b) cost breakdown of the optimal design of Case study 8 (α_{BD}=0.75, k_{f0}=8.41·10^6 m^3/(kmol·s) and K_{eq}=81).

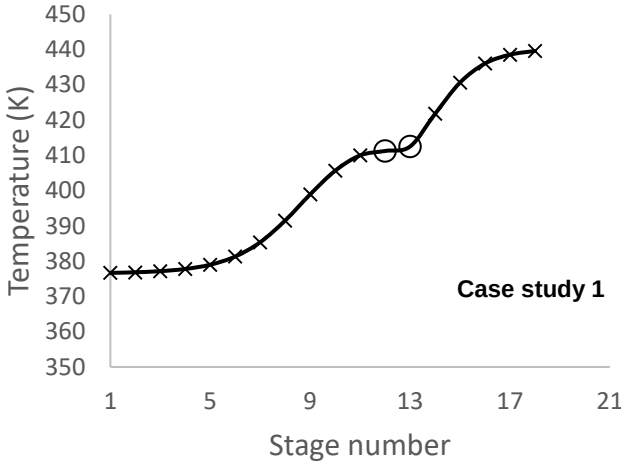
Temperature (K)
Stage number
Case study 1

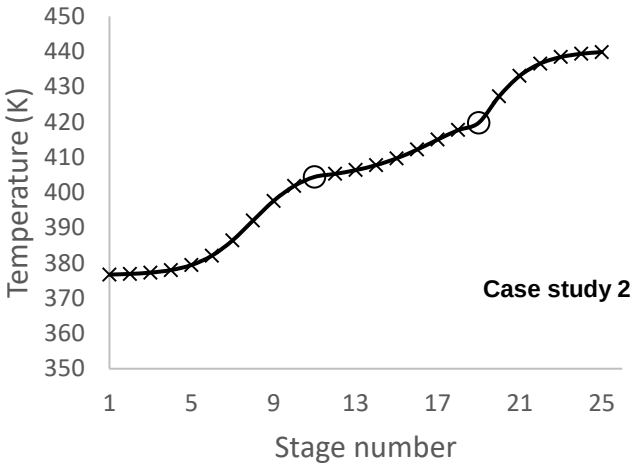
Temperature (K)
Stage number
Case study 2

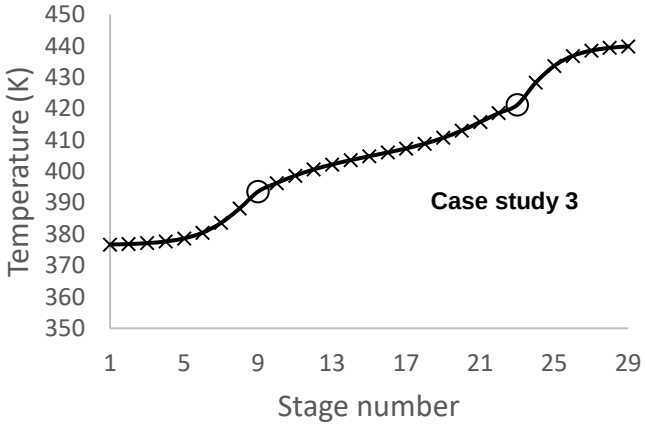
Temperature (K)
Stage number
Case study 3

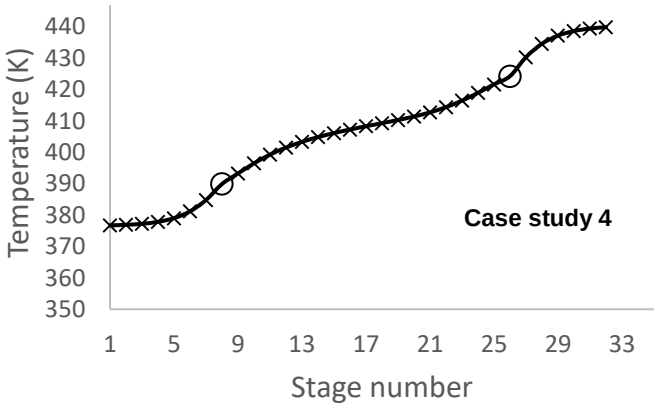
Temperature (K)
Stage number
Case study 4

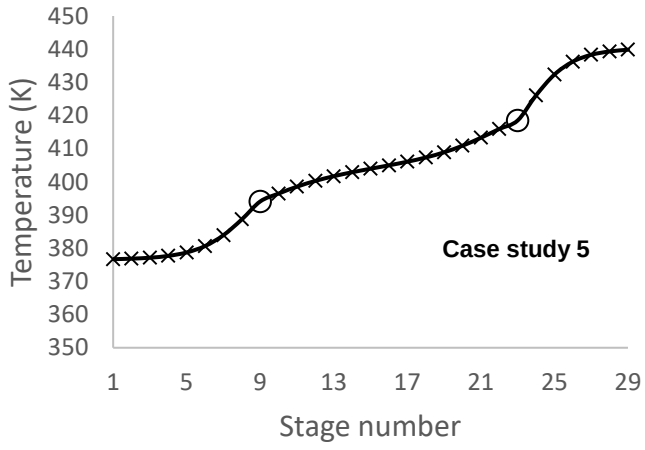
Temperature (K)
Stage number
Case study 5

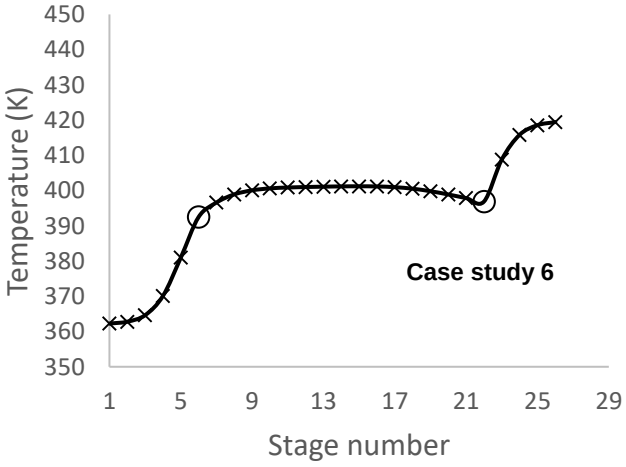
Temperature (K)
Stage number
Case study 6

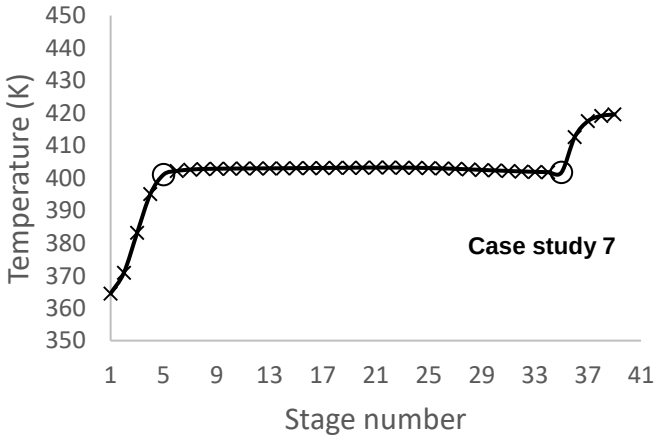
Temperature (K)
Stage number
Case study 7

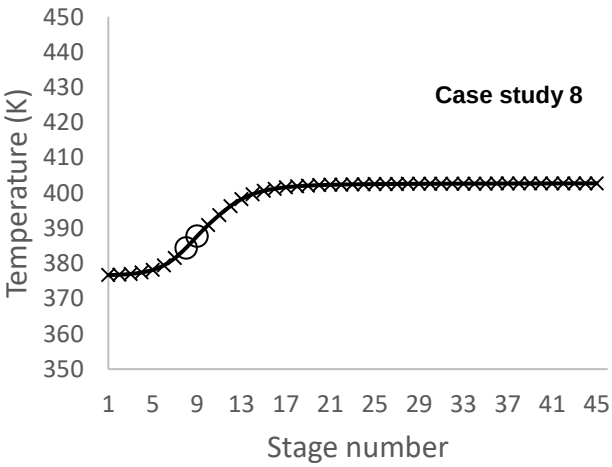
Temperature (K)
Stage number
Case study 8

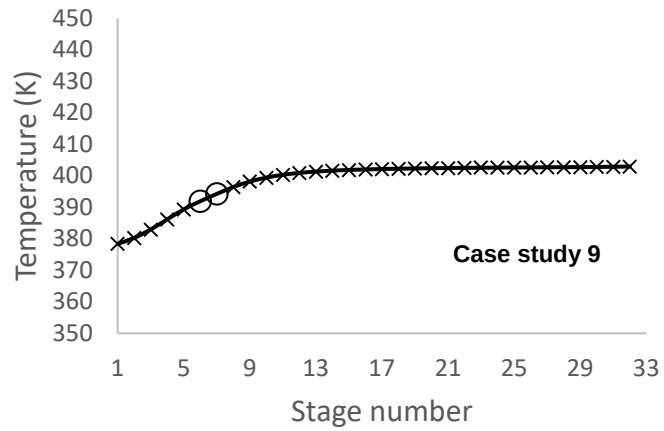

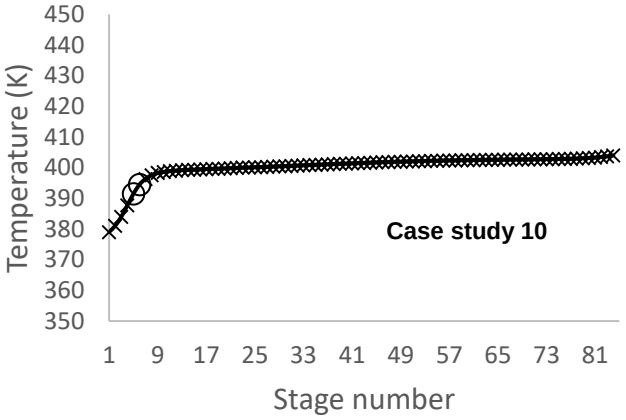

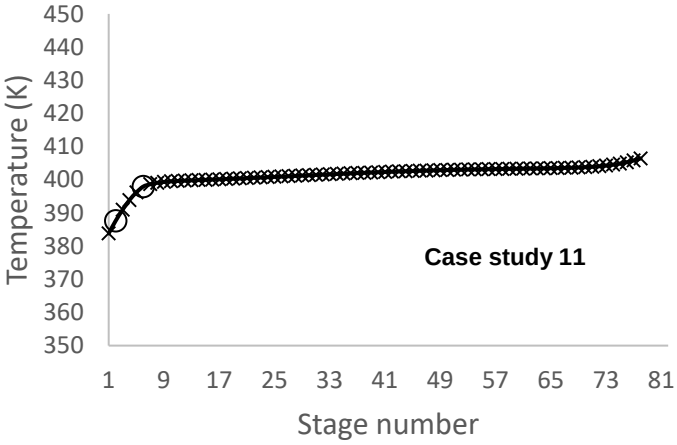

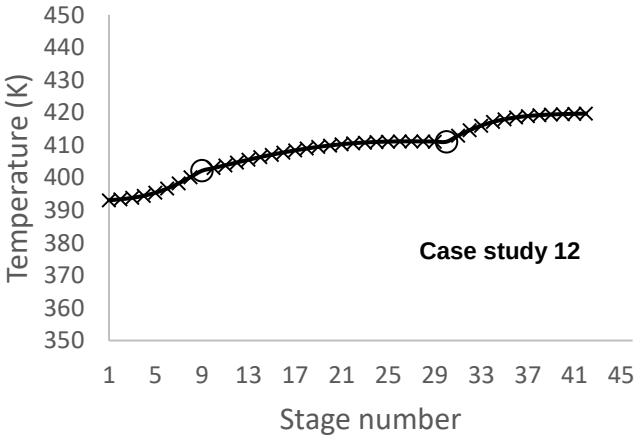

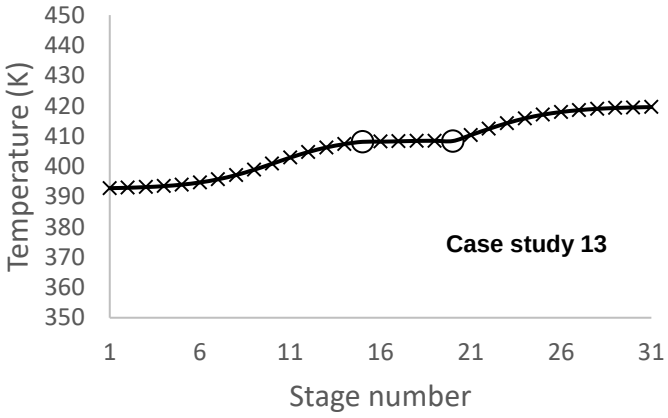

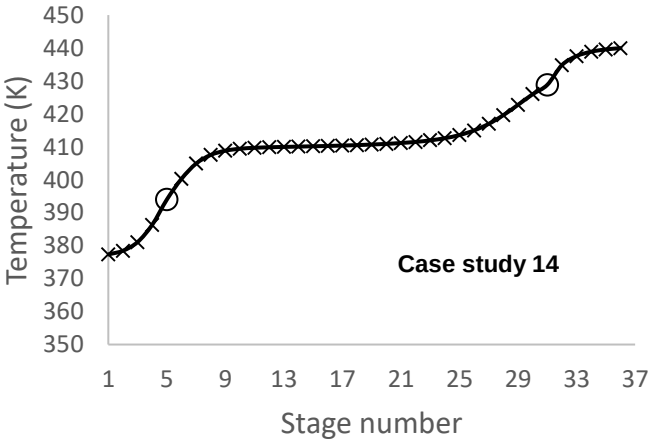

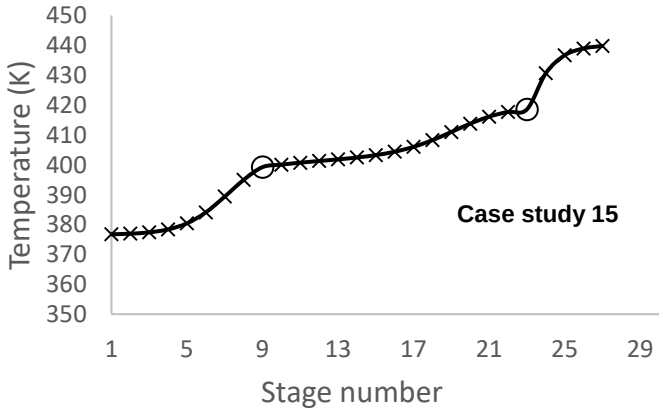

Figure 6: Temperature profiles of the optimal column designs for all case studies (feed locations are marked with "o", data in Table 2 to Table 4).

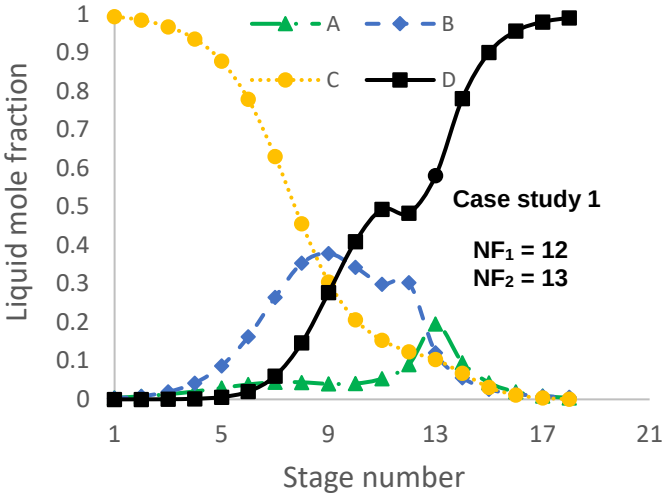
Liquid mole fraction
Stage number
A
B
C
D
Case study 1
NF₁ = 12
NF₂ = 13

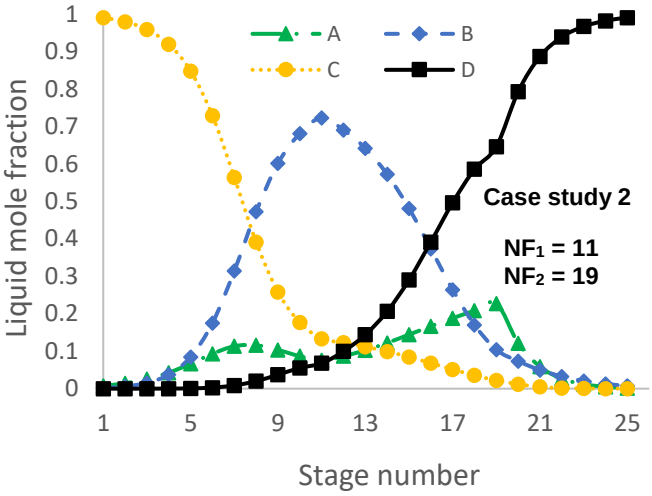
Liquid mole fraction
Stage number
A
B
C
D
Case study 2
NF₁ = 11
NF₂ = 19

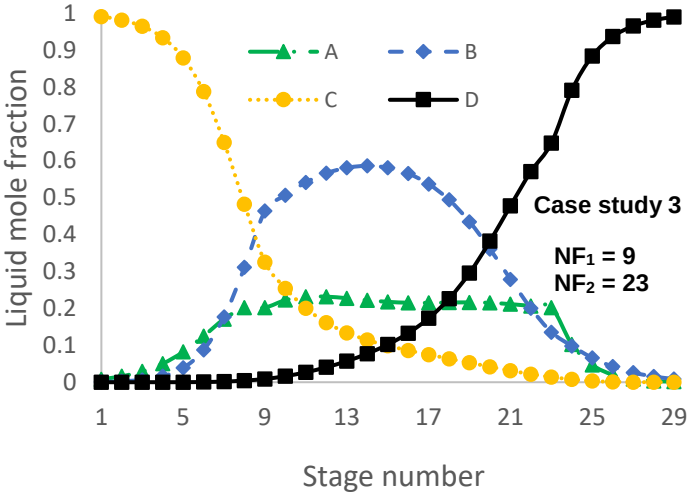
Liquid mole fraction
Stage number
A
B
C
D
Case study 3
NF₁ = 9
NF₂ = 23

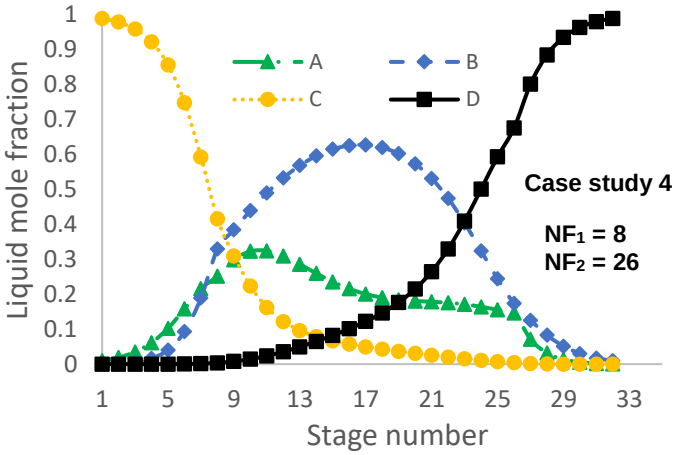
Liquid mole fraction
Stage number
A
B
C
D
Case study 4
NF₁ = 8
NF₂ = 26

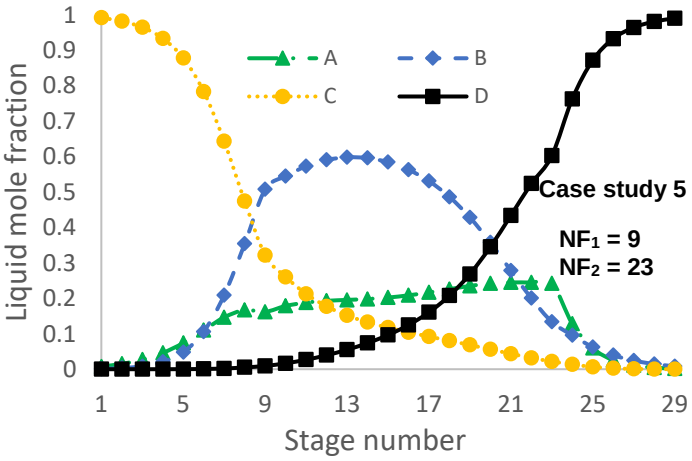
Liquid mole fraction
Stage number
A
B
C
D
Case study 5
NF₁ = 9
NF₂ = 23

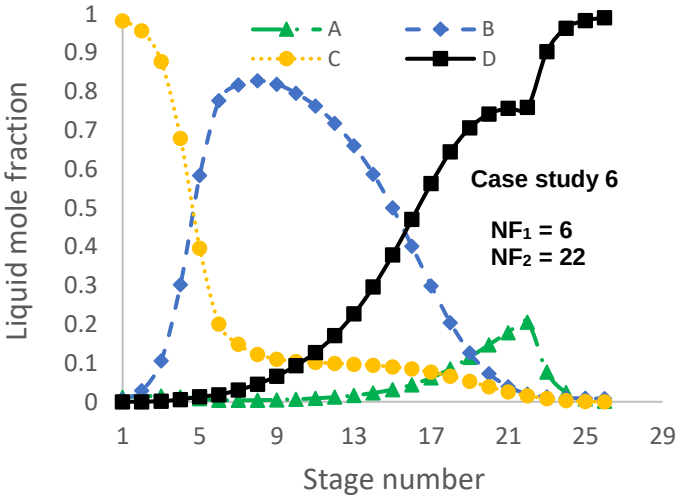
Liquid mole fraction
Stage number
A
B
C
D
Case study 6
NF₁ = 6
NF₂ = 22

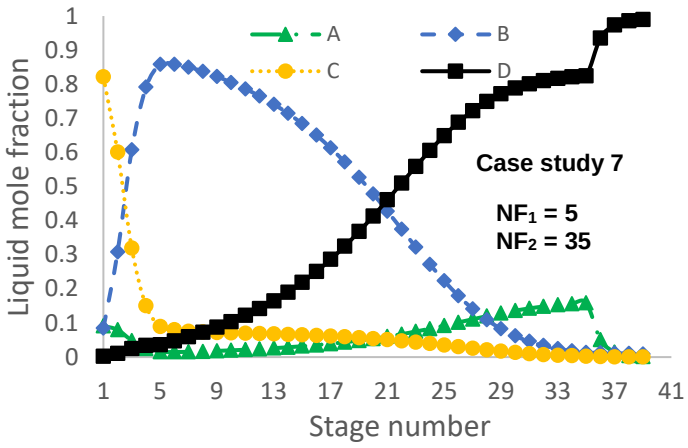
Liquid mole fraction
Stage number
A
B
C
D
Case study 7
NF1 = 5
NF2 = 35

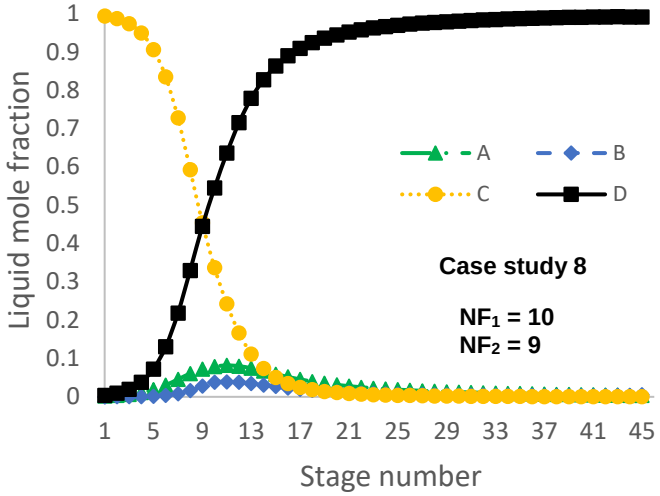
Liquid mole fraction
Stage number
A
B
C
D
Case study 8
NF1 = 10
NF2 = 9

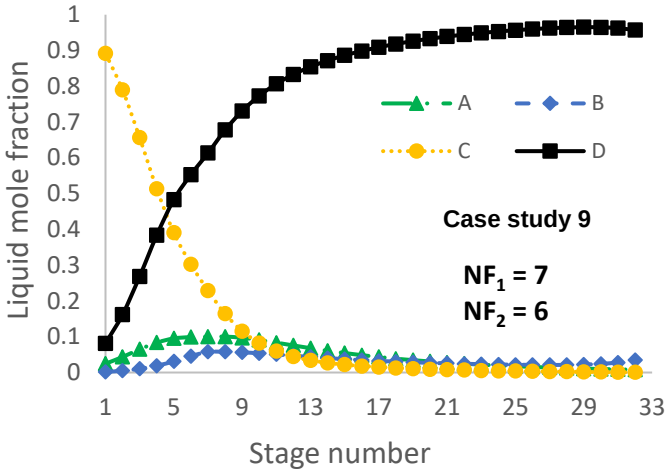
Liquid mole fraction
Stage number
A
B
C
D
Case study 9
NF1 = 7
NF2 = 6

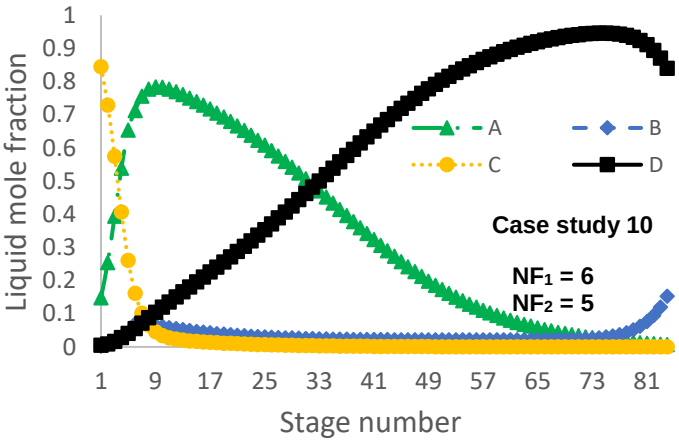
Liquid mole fraction
Stage number
A
B
C
D
Case study 10
NF1 = 6
NF2 = 5

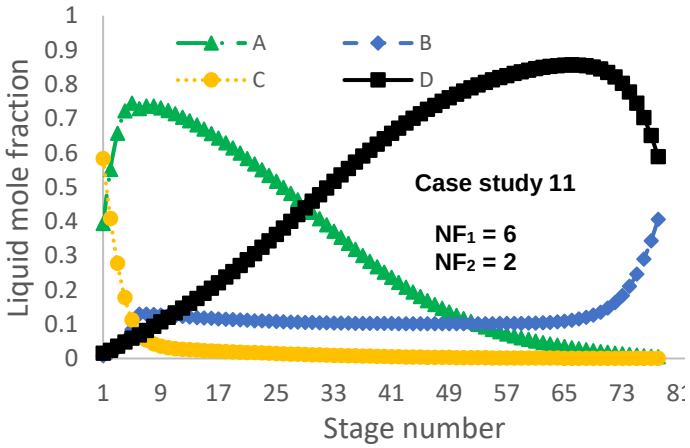
Liquid mole fraction
Stage number
A
B
C
D
Case study 11
NF1 = 6
NF2 = 2

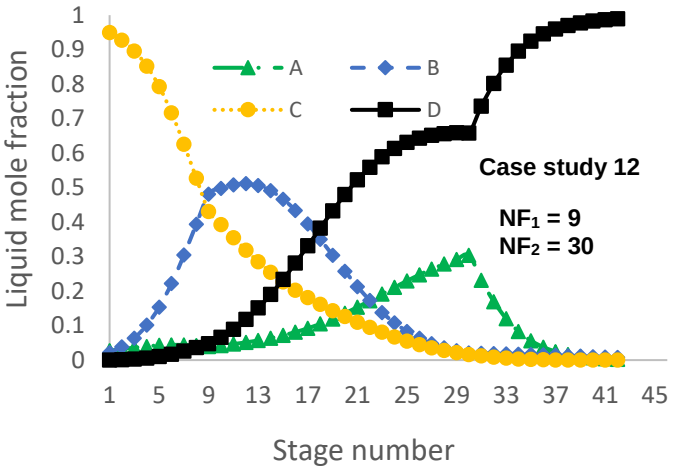
Liquid mole fraction
Stage number
A
B
C
D
Case study 12
NF1 = 9
NF2 = 30

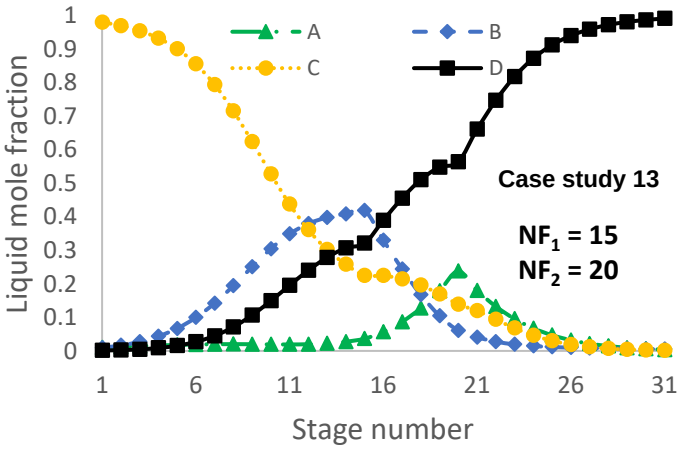
Liquid mole fraction
Stage number
A
B
C
D
Case study 13
NF1 = 15
NF2 = 20

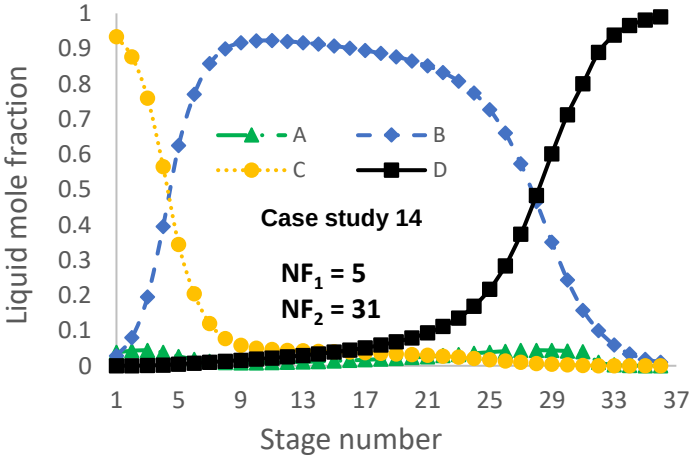
Liquid mole fraction
Stage number
A
B
C
D
Case study 14
NF1 = 5
NF2 = 31

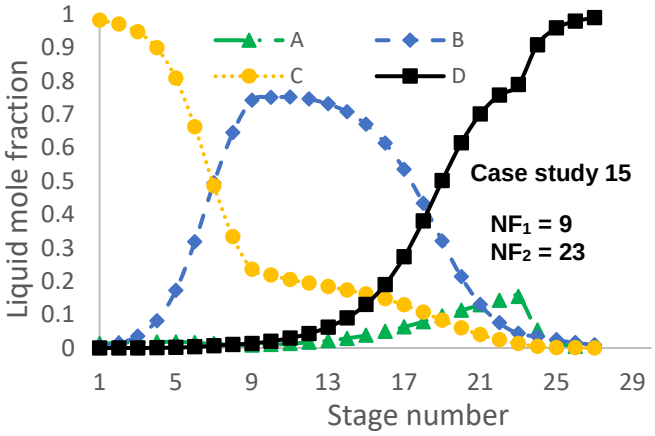

Figure 7: Composition profiles of the optimal column designs for all case studies (data in Table 2 to Table 4).

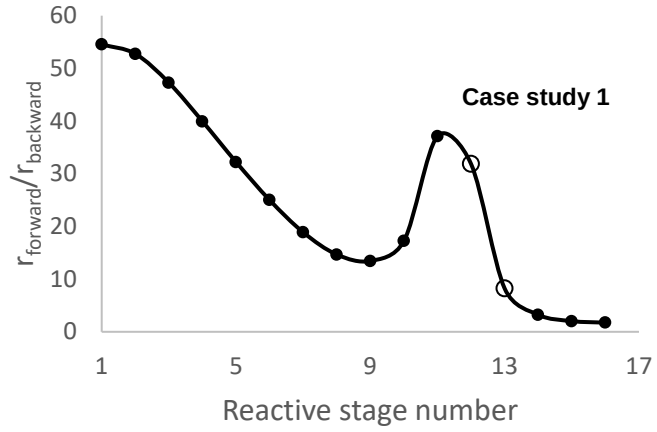
Case study 1
$r_{forward}/r_{backward}$
Reactive stage number

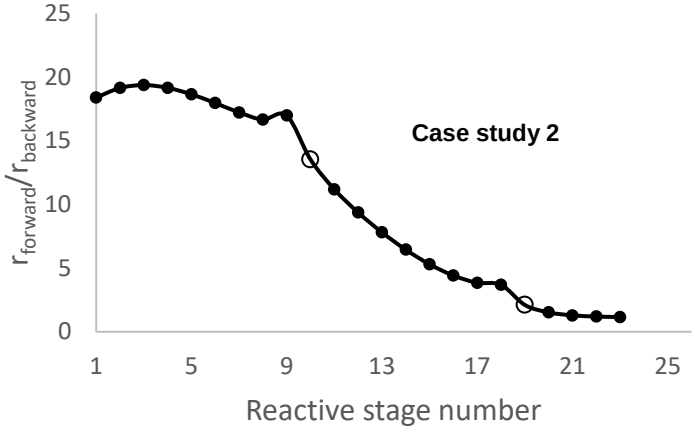
Case study 2
$r_{forward}/r_{backward}$
Reactive stage number

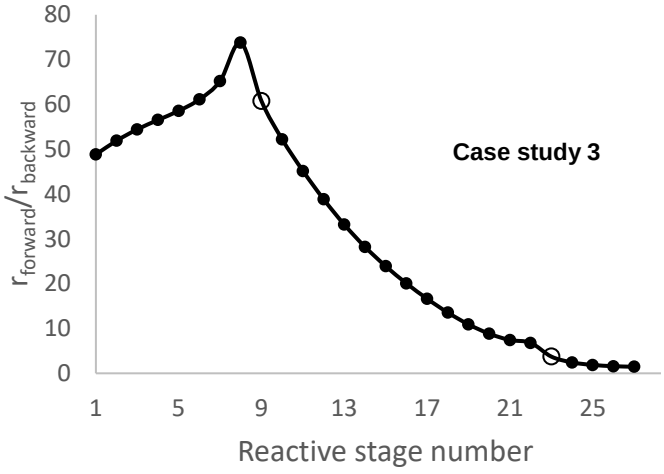
Case study 3
$r_{forward}/r_{backward}$
Reactive stage number

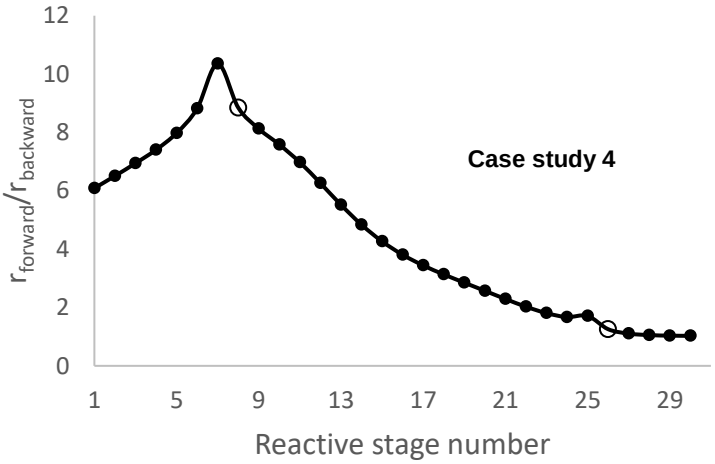
Case study 4
$r_{forward}/r_{backward}$
Reactive stage number

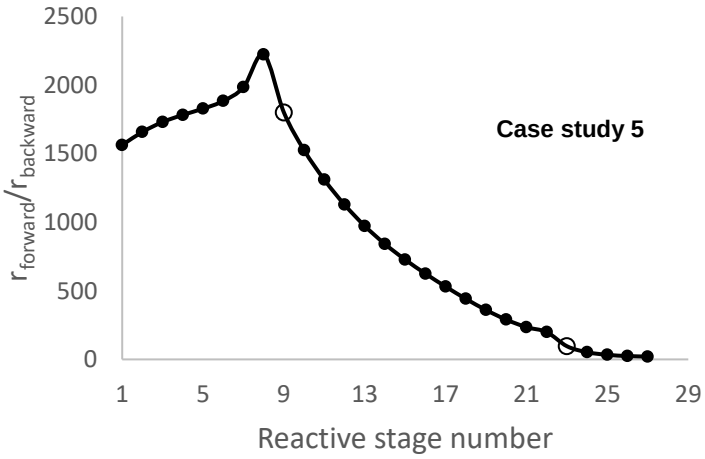
Case study 5
$r_{forward}/r_{backward}$
Reactive stage number

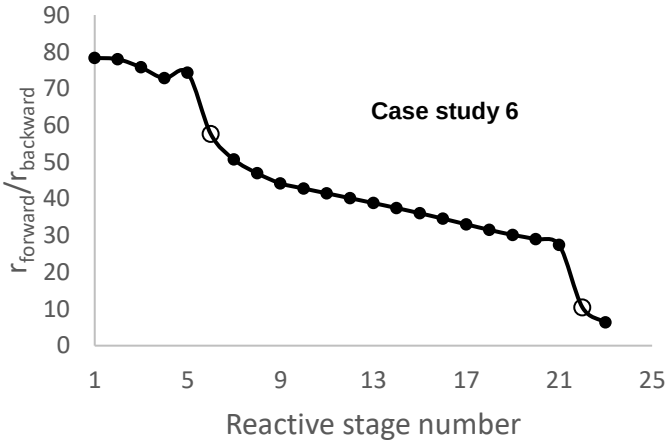
Case study 6
$r_{forward}/r_{backward}$
Reactive stage number

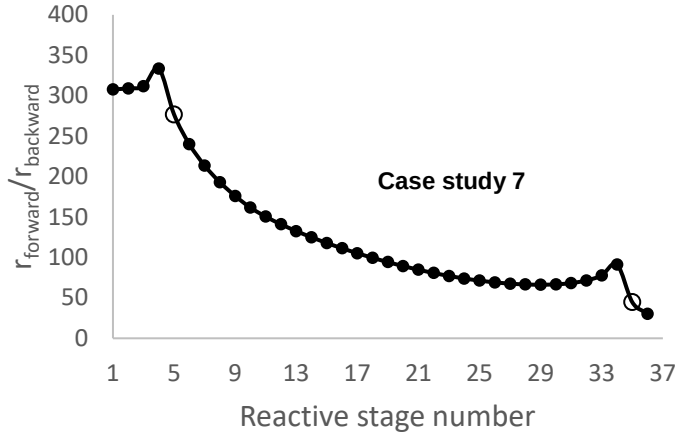
Case study 7
$r_{forward}/r_{backward}$
Reactive stage number

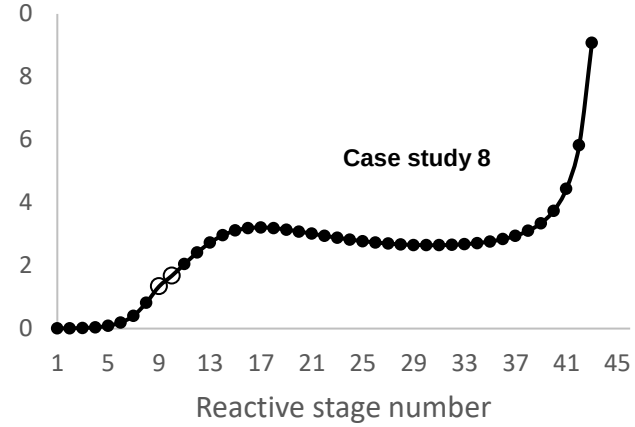
Case study 8
Reactive stage number

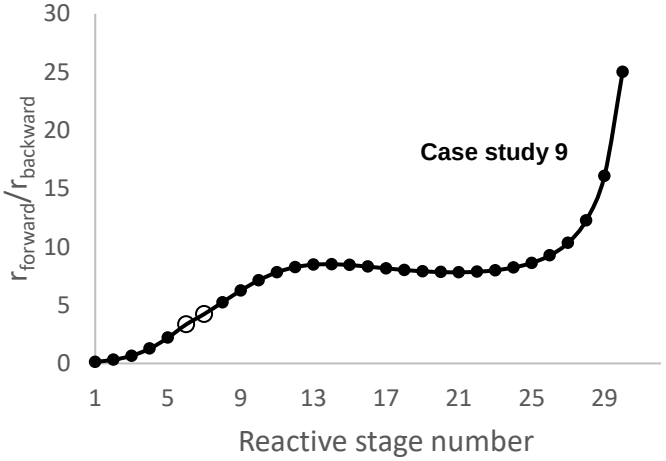
Case study 9
$r_{forward}/r_{backward}$
Reactive stage number

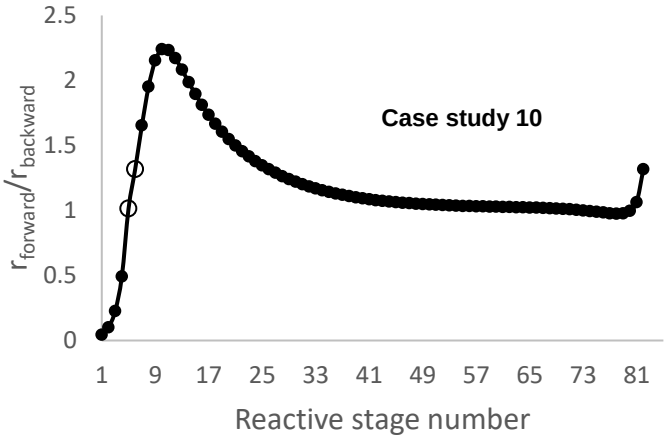
Case study 10
$r_{forward}/r_{backward}$
Reactive stage number

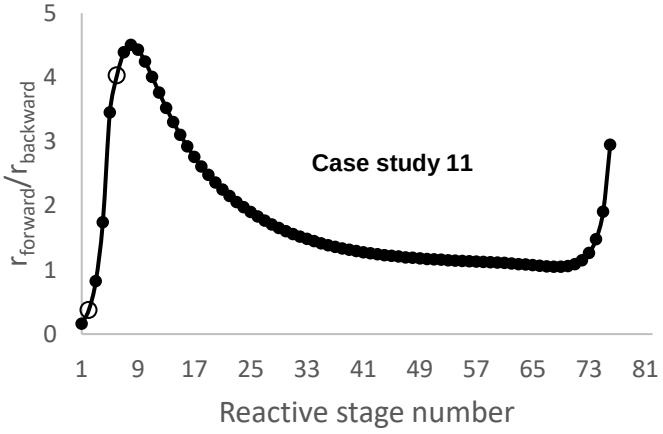
Case study 11
$r_{forward}/r_{backward}$
Reactive stage number

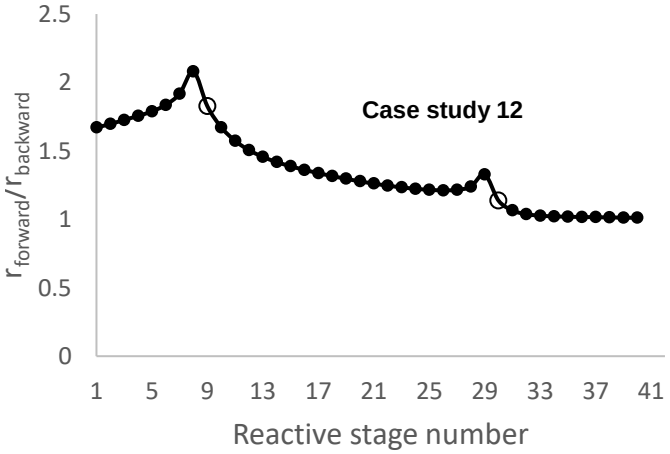
Case study 12
$r_{forward}/r_{backward}$
Reactive stage number

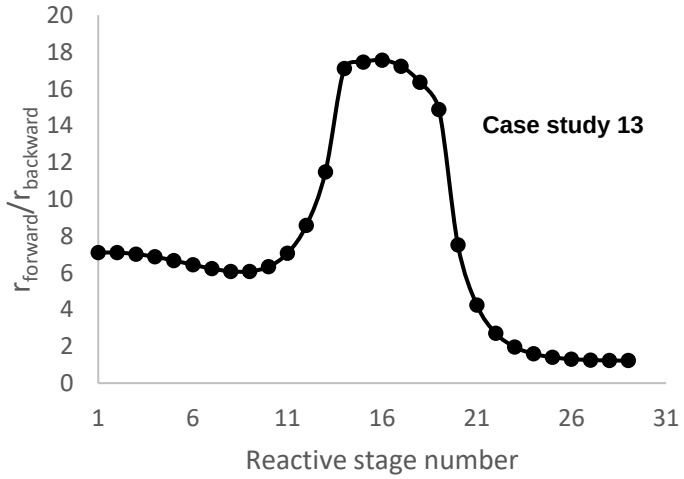
Case study 13
$r_{forward}/r_{backward}$
Reactive stage number

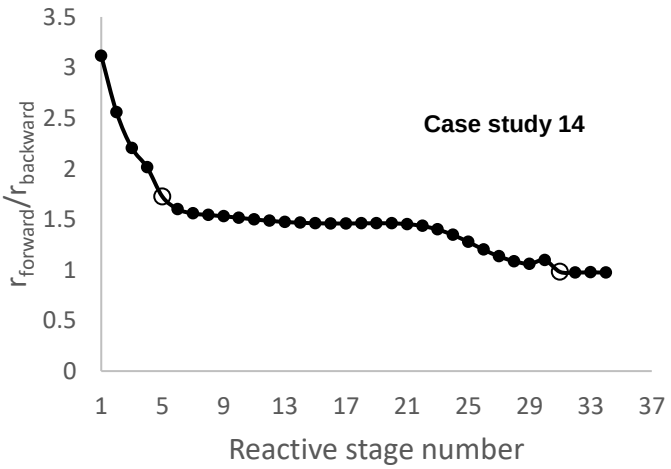
Case study 14
$r_{forward}/r_{backward}$
Reactive stage number

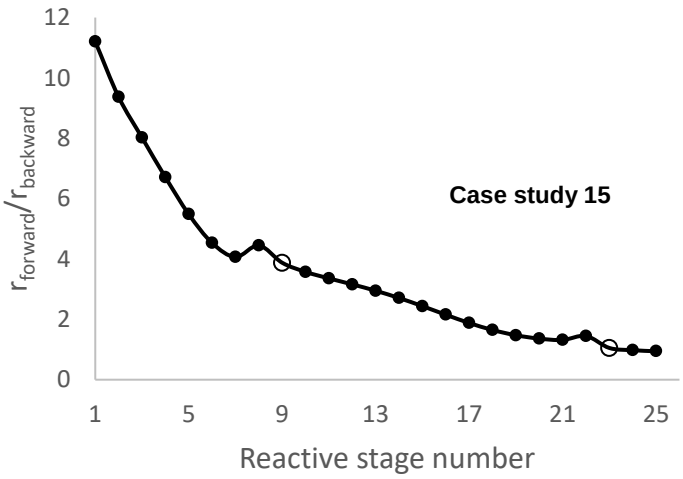

Figure 8: Forward to backward reaction rate ratio of the optimal column designs for all case studies (feed locations are marked with "o", data in Table 2~~Table 2~~ to Table 4~~Table 4~~).

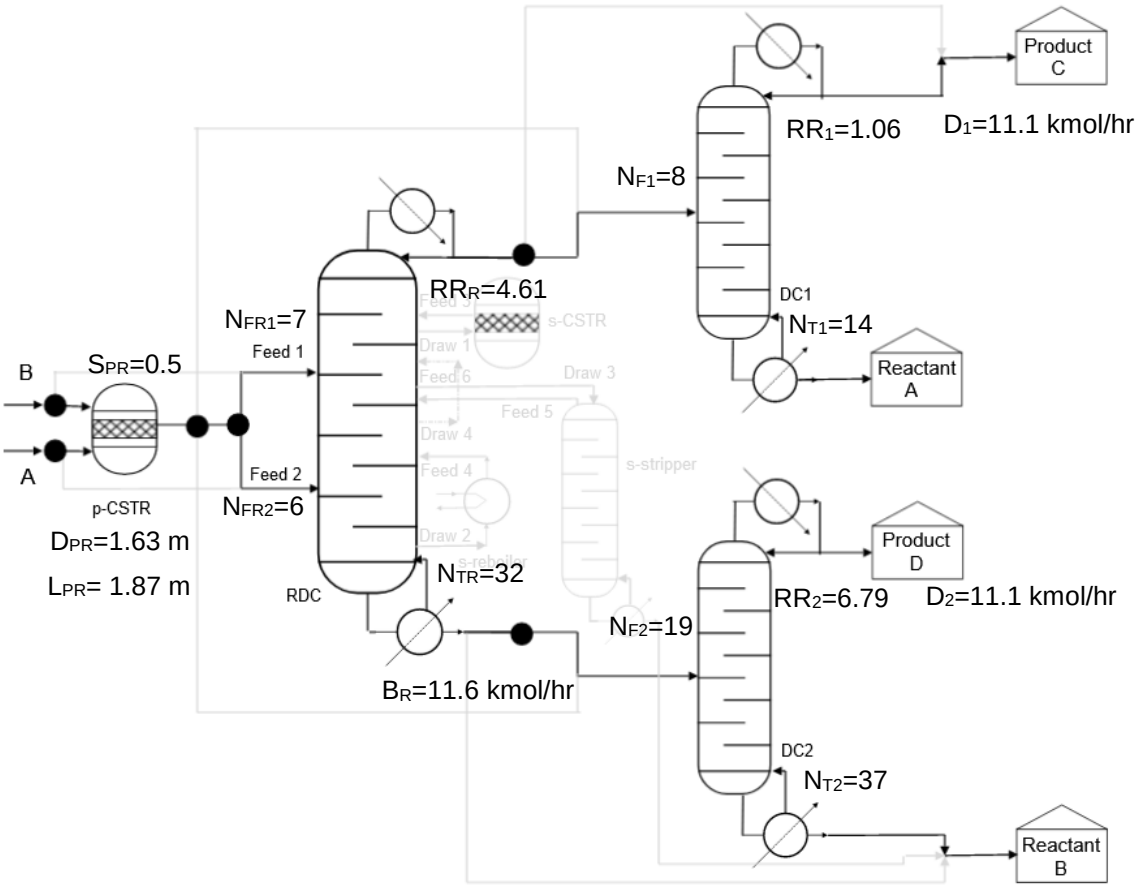

Figure 9: Optimal flowsheet for Case study 9. The optimal flowsheet is indicatively presented for this case study as the latter is characterised by the most complex design (pre-reactor, reactive distillation column, top and bottom conventional distillation columns).

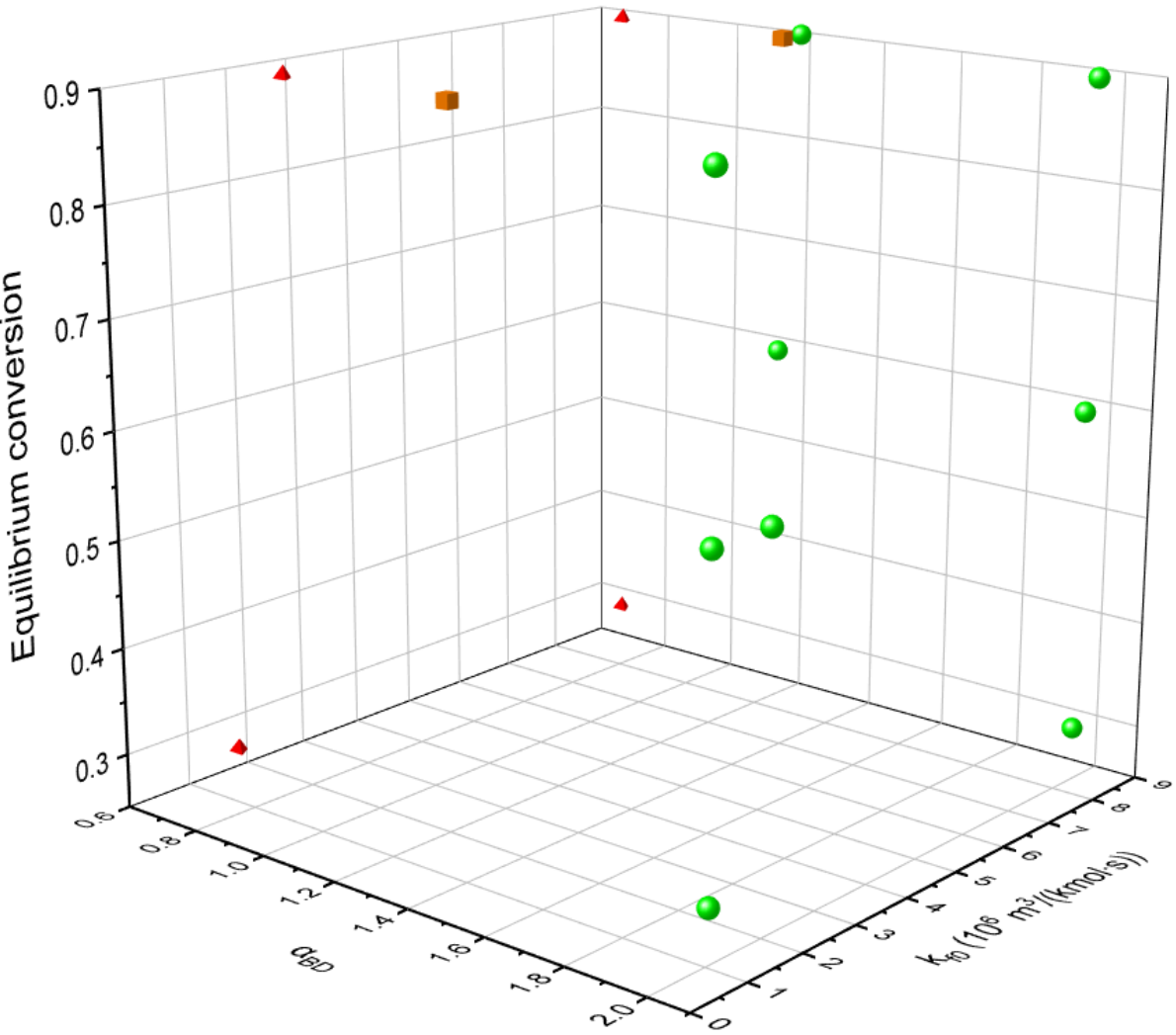

Figure 10: Optimal results for all case studies (Table 5 and Table 6) as a function of forward pre-exponential factor (k_{f0}), relative volatility between components B and D (α_{BD}), and equilibrium conversion (conversion of 0.3, 0.6 and 0.9 corresponds to K_{eq}=0.184, 2.25 and 81, respectively). ~~Points~~ Spheres marked green indicate cases studies with a single reactive distillation column; orange ~~points~~ cubes indicate case studies where the reactive column also requires a vapour pump-around stream; and red ~~points~~ tetrahedra indicate designs where a pre-reactor and/or additional columns were required for the optimal solution.

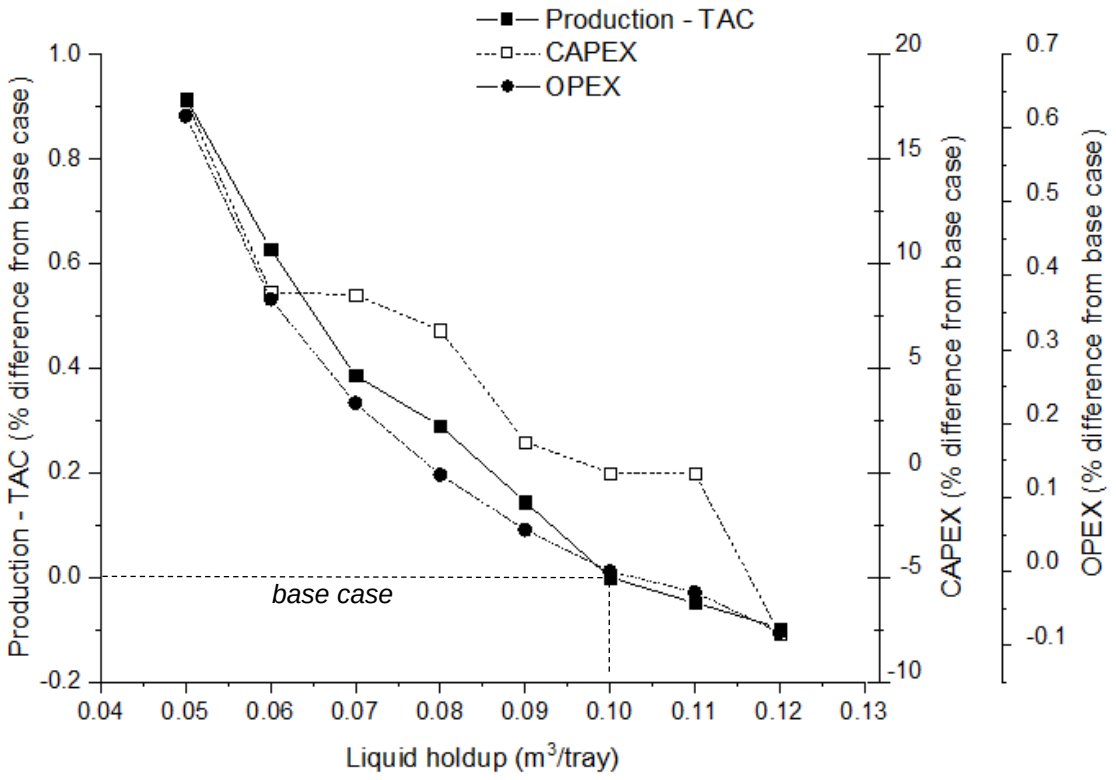

(a)

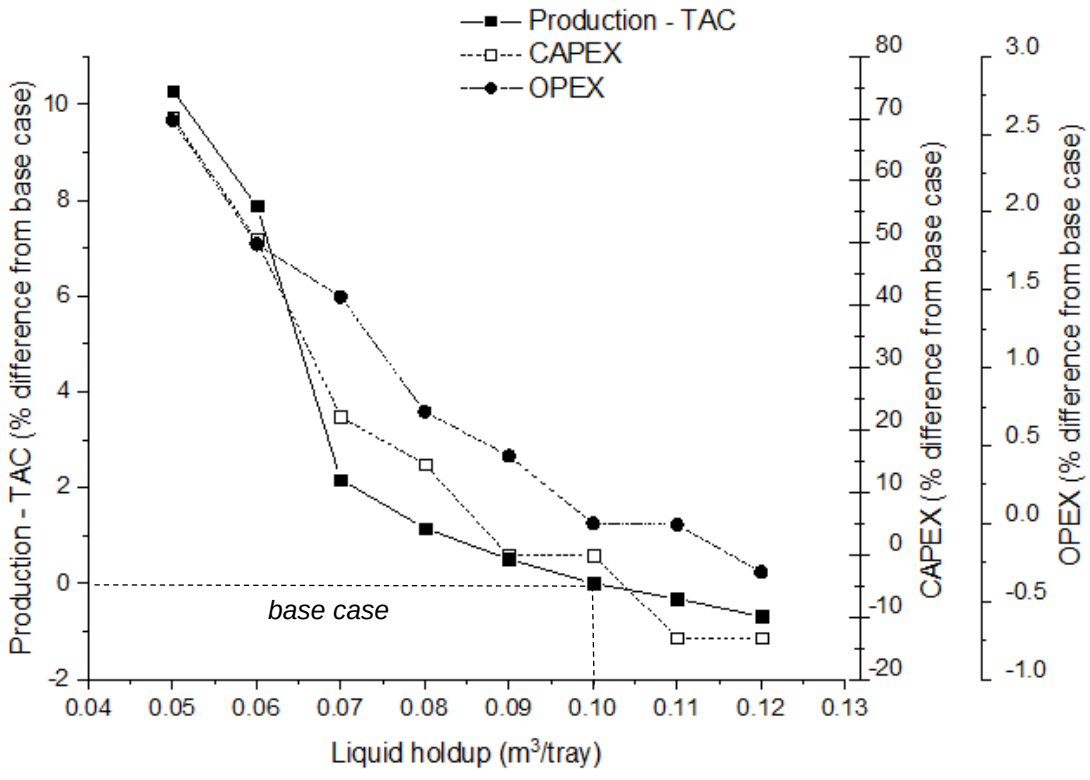

(b)

Figure 11: Optimal OPEX and CAPEX as a function of liquid holdup (data in Table 7), based on:
(a) Case study 1 (α_{BD}=2, k_{f0}=8.41·10^6 m^3/(kmol·s) and K_{eq}=81);
(b) Case study 5 (α_{BD}=2, k_{f0}=1.05·10^6 m^3/(kmol·s) and K_{eq}=81).

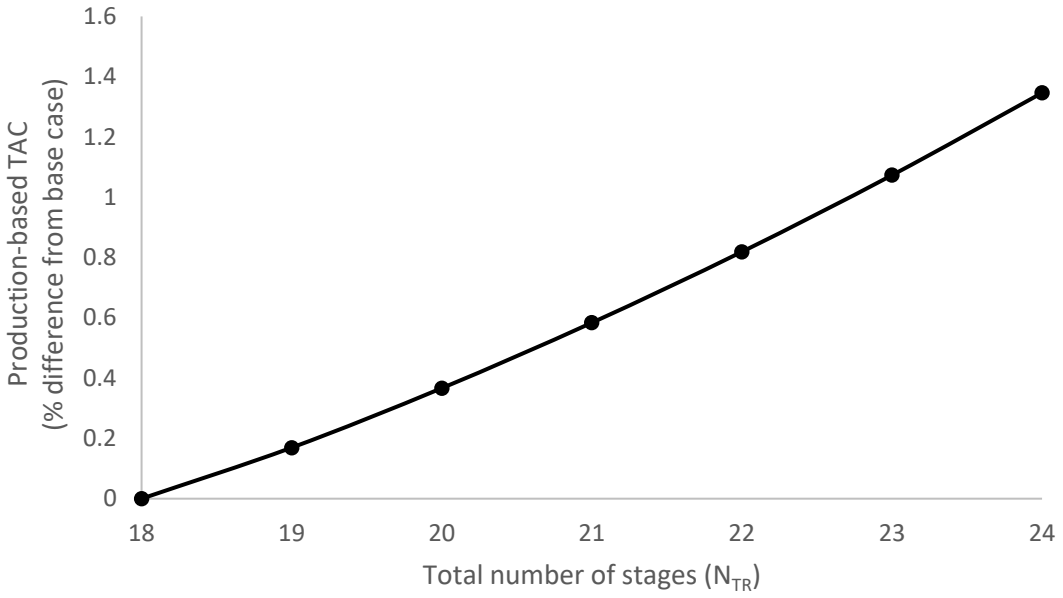

Figure 12a: Production-based TAC as a function of total number of stages, based on Case study 1 (α_{BD}=2, k_{f0}=8.41·10^6 m^3/(kmol·s) and K_{eq}=81). Base case of Case study 1 had N_{TR}=18.

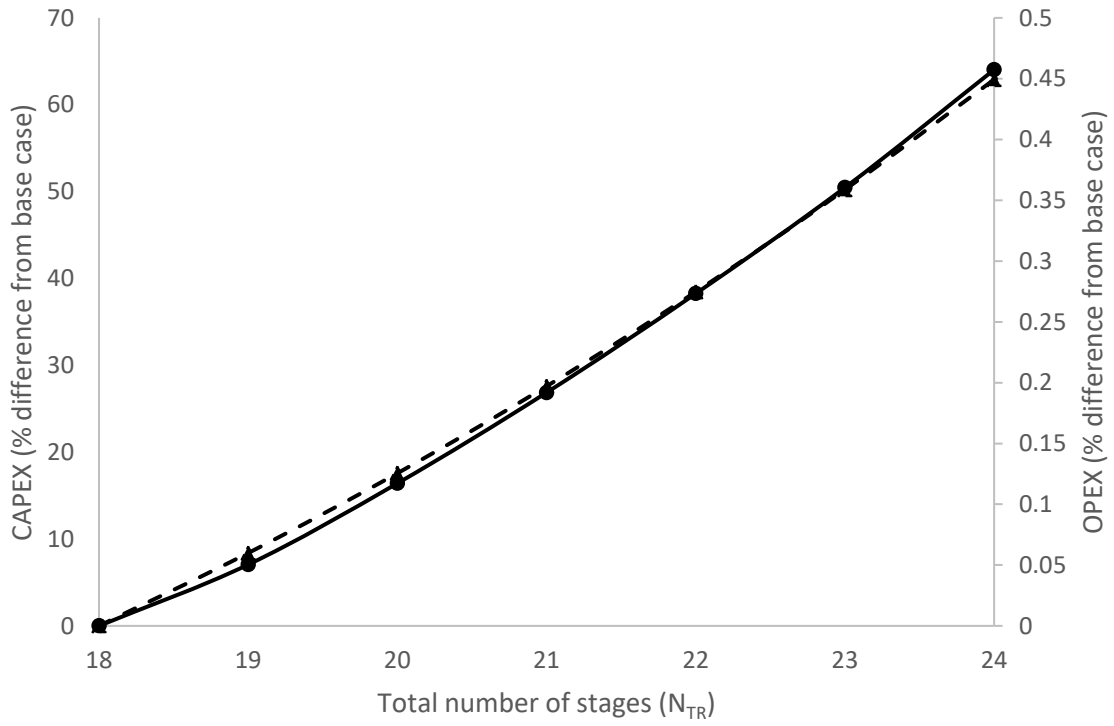

Figure 12b: CAPEX (left, dashed line) and OPEX (right, solid line) as a function of total number of stages, based on Case study 1 (α_{BD}=2, k_{f0}=8.41·10^6 m^3/(kmol·s) and K_{eq}=81). Base case of Case study 1 had N_{TR}=18.

Table 1: Superstructure decision variables considered.

Unit Variable	Symbol	Type
Reactive distillation column (RDC)		
Total number of stages[2]	N_{TR}	Integer
Feed 1 location (from p-CSTR or feedstock)	N_{FR1}	Integer
Feed 2 location (from p-CSTR or feedstock)	N_{FR2}	Integer
Feed 3 location (from s-CSTR)	N_{FR3}	Integer
Feed 4 location (from s-reboiler)	N_{FR4}	Integer
Feed 5 location (from s-stripper)	N_{FR5}	Integer
Feed 6 location (from vapour pump-around)	N_{FR6}	Integer
Draw 1 location (from RDC to s-CSTR)	N_{SR1}	Integer
Draw 2 location (from RDC to s-reboiler)	N_{SR2}	Integer
Draw 3 location (from RDC to s-stripper)	N_{SR3}	Integer
Draw 4 location (from RDC to vapour pump-around)	N_{SR4}	Integer
Draw 1 flow rate	S_{R1}	Continuous
Draw 2 flow rate	S_{R2}	Continuous
Draw 3 flow rate	S_{R3}	Continuous
Draw 4 flow rate	S_{R4}	Continuous
Reflux ratio (-)	RR_R	Continuous
Bottom flow rate (kmol/hr)	B_R	Continuous
Pre-reactor (p-CSTR)		
Reactor diameter (m)	D_{PR}	Continuous
Reactor length (m)	L_{PR}	Continuous
Outlet stream split	S_{PR}	Continuous
Side-reactor (s-CSTR)		
Reactor diameter (m)	D_{SR}	Continuous
Reactor length (m)	L_{SR}	Continuous
Top distillation column (DC1)		
Total number of stages	N_{T1}	Integer
Feed stage location	N_{F1}	Integer
Reflux ratio (-)	RR_1	Continuous
Distillate flow rate (kmol/hr)	D_1	Continuous
Bottom distillation column (DC2)		
Total number of stages	N_{T2}	Integer
Feed stage location	N_{F2}	Integer
Reflux ratio (-)	RR_2	Continuous
Distillate flow rate (kmol/hr)	D_2	Continuous
Side-stripper (s-stripper)		
Total number of stages	N_{FS}	Integer
Bottom flow rate (kmol/hr)	B_S	Continuous
Side-reboiler (s-reboiler)		
Reboiler heat duty (kW)	Q_{RB}	Continuous
Stream selection		
Feed 1 stream selection	S_{F1}	Binary (0 or 1)
Feed 2 stream selection	S_{F2}	Binary (0 or 1)
Top product stream selection	S_T	Binary (0 or 1)
Bottom product stream selection	S_B	Binary (0 or 1)
Reactive distillation column selection	S_R	Binary (0 or 1)
Side-stripper existence selection	S_S	Binary (0 or 1)
Side-reboiler existence selection	S_{RB}	Binary (0 or 1)
Side-reactor existence selection	S_{SR}	Binary (0 or 1)

Table 2: Case studies with different separation difficulty considered.

Relative volatility	**Value**	**Calculated boiling points (K)**
System I		
α_{CA} α_{AB} α_{BD}	2 1.5 2	T_C=376.6
		T_A=398.7
		T_B=413.0
		T_D=440.4
System II		
α_{CA} α_{AB} α_{BD}	1.2 4.15 1.2	T_C=362.1
		T_A=367.2
		T_B=413.0
		T_D=419.9
System III		
α_{CA} α_{AB} α_{BD}	2 1.5 0.75	T_C=376.6
		T_A=398.7
		T_D=402.7
		T_B=413.0
System IV		
α_{CA} α_{BA} α_{BD}	1.2 1.5 1.2	T_C=392.6
		T_A=398.7
		T_B=413.0
		T_D=419.9
System V		
α_{CA} α_{AB} α_{BD}	1.2 2.5 2	T_C=376.6
		T_A=382.2
		T_B=413.0
		T_D=440.4

[2]Note that in the reactive distillation column, all stages (Stage 2 to N_{TR}-1) were considered reactive and thus, the manipulation of the total number of stages automatically affects the length of the reactive zone.
Also, in gPROMS ProcessBuilder, Stage 1 is the condenser and Stage N_T is the reboiler, and stage numbering takes place from the top to the bottom.

Table 3: Separation/reaction parameters for all case studies.

	System (Table 2~~Table 2~~)	Relative volatility (Table 2)	k_{f0} (m^3/kmol·s)	K_{eq}
Case study 1	I	α_{CA}=2 α_{AB}=1.5 α_{BD}=2	$8.41 \cdot 10^6$	81
Case study 2			$2.10 \cdot 10^6$	2.25
Case study 3			$1.05 \cdot 10^6$	2.25
Case study 4			$1.05 \cdot 10^6$	0.184
Case study 5			$1.05 \cdot 10^6$	81
Case study 6	II	α_{CA}=1.2 α_{AB}=4.15 α_{BD}=1.2	$8.41 \cdot 10^6$	81
Case study 7			$2.10 \cdot 10^6$	81
Case study 8	III	α_{CA}=2 α_{AB}=1.5 α_{BD}=0.75	$8.41 \cdot 10^6$	81
Case study 9			$2.10 \cdot 10^6$	81
Case study 10			$8.41 \cdot 10^6$	0.184
Case study 11			$1.05 \cdot 10^6$	0.184
Case study 12	IV	α_{CA}=1.2 α_{AB}=1.5 α_{BD}=1.2	$8.41 \cdot 10^6$	2.25
Case study 13			$8.41 \cdot 10^6$	81
Case study 14	V	α_{CA}=1.2 α_{AB}=2.5 α_{BD}=2	$8.41 \cdot 10^6$	0.184
Case study 15			$8.41 \cdot 10^6$	2.25

Formatte

Table 4: Initial variable guesses for all case studies.

Reactive distillation column (RDC)	**Initial value**	**Minimum bound**	**Maximum bound**
Total number of stages	100	3	100
Feed 1 location (from p-CSTR or feed-stock)	5	2	99
Feed 2 location (from p-CSTR or feed-stock)	25	2	99
Feed 3 location (from s-CSTR)	28	2	99
Feed 4 location (from s-reboiler)	34	2	99
Feed 5 location (from s-stripper)	35	2	99
Feed 6 location (from vapour pump-around)	10	2	99
Draw 1 location (from RDC to s-CSTR)	10	2	99
Draw 2 location (from RDC to s-reboiler)	25	2	99
Draw 3 location (from RDC to s-stripper)	26	2	99
Draw 4 location (from RDC to vapour pump-around)	25	2	99
Draw 1 flow rate (kmol/hr)	0	0.0	5.0
Draw 2 flow rate (kmol/hr)	4.2	0.0	5.0
Draw 3 flow rate (kmol/hr)	4.2	0.0	5.0
Draw 4 flow rate (kmol/hr)	0.5	0.0	5.0
Reflux ratio (-)	2.0	0.1	40.0
Bottom flow rate (kmol/hr)	12.6	5.0	18.0
Pre-reactor (p-CSTR)			
Reactor diameter (m)	1.0	0.0	5
Reactor length (m)	1.0	0.0	5
Outlet stream split	0.0	0.0	1.0
Side-reactor (s-CSTR)			
Reactor diameter (m)	1.0	0.0	5
Reactor length (m)	1.0	0.0	5
Top distillation column (DC1)			
Total number of stages	50	3	50
Feed stages location	24	2	49
Reflux ratio (-)	5.9	0.1	15.0
Distillate flow rate (kmol/hr)	12.6	5.0	18.0
Bottom distillation column (DC2)			
Total number of stages	50	3	50
Feed stages location	24	2	49
Reflux ratio (-)	1.0	0.1	15.0
Distillate flow rate (kmol/hr)	12.6	0.6	18.0
Side-stripper (s-stripper)			
Total number of stages	10	2	10
Bottom flow rate (kmol/hr)	1.8	0.0	5.0
Side-reboiler (s-reboiler)			
Reboiler heat duty (kW)	0.0	0.0	500.0
Stream selection			
Feed 1 stream selection	1	0	1
Feed 2 stream selection	1	0	1
Top product stream selection	1	0	1
Bottom product stream selection	0	0	1
Reactive distillation column selection	1	0	1
Side-stripper existence selection	1	0	1
Side-reboiler existence selection	0	0	1
Side-reactor existence selection	0	0	1

Table 5: Optimal results for all case studies considered.

	CASE STUDIES														
Variable	**1**	**2**	**3**	**4**	**5**	**6**	**7**	**8**	**9**	**10**	**11**	**12**	**13**	**14**	**15**
α_{CA}- α_{AB}- α_{BD}[3]	2-1.5-2	2-1.5-2	2-1.5-2	2-1.5-2	2-1.5-2	1.2-4.15-1.2	1.2-4.15-1.2	2-1.5-0.75	2-1.5-0.75	2-1.5-0.75	2-1.5-0.75	1.2-1.5-1.2	1.2-1.5-1.2	1.2-2.5-2	1.2-2.5-2
System (Table 2)	I					II		III				IV		V	
k_{f0} (m^3/(kmol·s))[4]	$8.41\cdot10^6$	$2.1\cdot10^6$	$1.05\cdot10^6$	$1.05\cdot10^6$	$1.05\cdot10^6$	$8.41\cdot10^6$	$2.1\cdot10^6$	$8.41\cdot10^6$	$2.1\cdot10^6$	$8.41\cdot10^6$	$1.05\cdot10^6$	$8.41\cdot10^6$	$8.41\cdot10^6$	$8.41\cdot10^6$	$8.41\cdot10^6$
K_{eq}[4]	81	2.25	2.25	0.184	81	81	81	81	81	0.184	0.184	2.25	81	0.184	2.25
	Optimal results														
RR_R	2.59	4.65	5.76	7.97	5.09	3.07	3.13	6.99	4.61	36.72	18.24	8.32	6.2	10.66	3.70
B_R (kmol/hr)	12.6	12.6	12.6	12.6	12.6	12.6	11.4	12.6	11.6	12.6	12.4	12.3	12.5	12.2	12.6
N_{FR1}	12	11	9	8	9	6	5	10	7	6	6	9	15	5	9
N_{FR2}	13	19	23	26	23	22	35	9	6	5	2	30	20	31	23
N_{FR6}	-	-	-	-	-	10	11	-	-	-	-	-	-	-	-
N_{SR4}	-	-	-	-	-	25	33	-	-	-	-	-	-	-	-
N_{TR}	18	25	29	32	29	26	39	45	32	85	78	42	31	36	27
$x_{D,A}$	0.004	0.007	0.008	0.009	0.008	0.012	0.091	0.002	0.025	0.148	0.394	0.027	0.011	0.038	0.013
$x_{D,B}$	0.003	0.002	0.001	0.001	0.001	0.006	0.085	Trace	0.002	0.002	0.008	0.022	0.009	0.029	0.005
$x_{D,C}$	0.993	0.991	0.991	0.990	0.991	0.982	0.822	0.994	0.892	0.845	0.583	0.950	0.979	0.933	0.982
$x_{D,D}$	Trace	trace	Trace	Trace	Trace	Trace	0.002	0.004	0.081	0.005	0.015	0.001	0.001	Trace	Trace
$x_{B,A}$	0.004	0.002	0.001	0.001	0.002	0.002	0.001	0.004	0.008	0.007	0.005	0.002	0.004	Trace	0.001
$x_{B,B}$	0.005	0.007	0.009	0.009	0.008	0.008	0.009	0.005	0.035	0.153	0.406	0.008	0.005	0.01	0.009
$x_{B,C}$	0.001	trace	Trace	Trace	Trace	Trace	Trace	Trace	Trace	Trace	Trace	Trace	0.001	Trace	Trace
$x_{B,D}$	0.990	0.991	0.990	0.990	0.990	0.990	0.990	0.991	0.957	0.840	0.589	0.990	0.990	0.990	0.990
D_{PR} (m)	-	-	-	-	-	-	-	1.12	1.63	-	-	-	-	-	-
L_{PR} (m)	-	-	-	-	-	-	-	1.93	1.87	-	-	-	-	-	-
S_{PR}	-	-	-	-	-	-	-	0.5	0.5	-	-	-	-	-	-
S_{R4} (kmol/hr)	-	-	-	-	-	0.1	0.1	-	-	-	-	-	-	-	-
RR_1	-	-	-	-	-	-	-	-	1.06	1.35	2.93	-	-	-	-
D_1 (kmol/hr)	-	-	-	-	-	-	-	-	11.1	9.7	6.8	-	-	-	-
N_1	-	-	-	-	-	-	-	-	8	12	14	-	-	-	-

[3] The relative volatilities of all case studies are presented in Table 2~~Table 2~~.

[4] The kinetic parameters of all case studies are presented in Table 3.

N_{T1}	-	-	-	-	-	-	-	-	14	17	17	-	-	-	-
RR_2	-	-	-	-	-	-	-	-	6.79	8.95	13.76	-	-	-	-
D_2 (kmol/hr)	-	-	-	-	-	-	-	-	11.1	10.6	7.3	-	-	-	-
N_2	-	-	-	-	-	-	-	-	19	27	29	-	-	-	-
N_{T2}	-	-	-	-	-	-	-	-	37	44	47	-	-	-	-
x_{REC}	1.00	1.00	1.00	1.00	1.00	1.00	1.00	1.00	0.90	0.98	0.96	1.00	1.00	1.00	1.00
$x_{B,D}$	0.99	0.99	0.99	0.99	0.99	0.99	0.99	0.99	0.99	0.99	0.99	0.99	0.99	0.99	0.99
Q_C (kW)	-341.3	-537.9	-643.1	-853.6	-578.8	-404.8	-454.2	-763.3	-600.8	-3539.1	-1792.0	-864.5	-657.6	-1145.1	-448.6
Q_R (kW)	227.9	424.7	530.0	740.5	466.2	284.6	344.1	637.9	479.6	3433.1	1717.8	757.4	549.2	1039.9	340.7
d_R (diameter, m)	0.62	0.78	0.85	0.99	0.81	0.64	0.65	0.93	0.77	1.98	1.39	1.04	0.91	1.13	0.71
d_1 (diameter, m)	-	-	-	-	-	-	-	-	0.43	0.44	0.48	-	-	-	-
d_2 (diameter, m)	-	-	-	-	-	-	-	-	0.79	0.96	1.00	-	-	-	-
Production - TAC (€/kg)[5]	2.073	2.140	2.178	2.231	2.168	2.138	2.541	2.389	2.963	4.861	6.480	2.390	2.210	2.390	2.150
OPEX (M€/yr)	10.32	10.52	10.63	10.82	10.59	10.44	10.89	11.03	11.83	15.77	14.44	11.04	10.68	11.15	10.49
CAPEX (M€/yr)	0.15	0.27	0.35	0.43	0.35	0.29	0.71	1.00	1.28	4.80	4.44	0.76	0.40	0.55	0.31

[5] The objective function was calculated in €/ktn but is shown in €/kg to avoid a large number of decimals.

Table 6: Optimal results for all case studies as illustrated in Figure 10.

Case study	**1**	**2**	**3**	**4**	**5**	**6**	**7**	**8**	**9**	**10**	**11**	**12**	**13**	**14**	**15**
α_{BD}	2	2	2	2	2	1.2	1.2	0.75	0.75	0.75	0.75	1.2	1.2	2	2
k_{f0} ($\cdot 10^6$) (m^3/(kmol·s))	8.41	2.1	1.05	1.05	1.05	8.41	2.1	8.41	2.1	8.41	1.05	8.41	8.41	8.41	8.41
K_{eq}	81	2.25	2.25	0.184	81	81	81	81	81	0.184	0.184	2.25	81	0.184	2.25
Conversion[6]	0.9	0.6	0.6	0.3	0.9	0.9	0.9	0.9	0.9	0.3	0.3	0.6	0.9	0.3	0.6
Optimal design															
RDC	×	×	×	×	×	×	×	×	×	×	×	×	x	×	×
p-CSTR								×	×						
DC1									×	×	×				
DC2									×	×	×				
Vapour pump-around stream						×	×								

[6] K_{eq} can be calculated based on the desired conversion ([D]/[A_0]=0.3, 0.6 or 0.9) at reaction equilibrium. In addition, k_{f0} can be calculated using the following equation for a batch reactor: $k_{f0} * t = \frac{conversion}{(1-conversion)*[A_0]}$ where t is the time required for the reaction to reach 90% conversion, taken in this work as 15, 60 or 120 min for k_{f0}= 8.41·10^6, 2.1·10^6, 1.05·10^6 m^3/(kmol·s), respectively.

Table 7: Optimal design results as a function of liquid holdup based on: (a) Case study 1 and (b) Case study 5 as the base cases.

(a)

	Liquid holdup (h, m^3/tray)							
Variable	**0.05**	**0.06**	**0.07**	**0.08**	**0.09**	**0.10***	**0.11**	**0.12**
RR_R	3.35	3.04	2.84	2.76	2.66	2.59	2.54	2.52
B_R (kmol/hr)	12.6	12.6	12.6	12.6	12.6	12.6	12.6	12.6
N_{FR1}	13	13	13	12	12	12	12	11
N_{FR2}	15	14	14	13	13	13	13	12
N_{TR}	20	19	19	18	18	18	18	17
Production-based TAC (€/kg)	2.092	2.086	2.081	2.079	2.076	2.073	2.072	2.071
CAPEX (M€/yr)	0.18	0.16	0.16	0.16	0.15	0.15	0.15	0.14
OPEX (M€/yr)	10.38	10.36	10.34	10.33	10.33	10.32	10.32	10.31

*Base case

(b)

	Liquid holdup (h, m^3/tray)							
Variable	**0.05**	**0.06**	**0.07**	**0.08**	**0.09**	**0.10***	**0.11**	**0.12**
RR_R	5.33	5.00	6.64	5.86	5.79	5.09	5.43	4.95
B_R (kmol/hr)	12.0	12.1	12.6	12.6	12.6	12.6	12.6	12.6
N_{FR1}	8	9	8	7	9	9	7	10
N_{FR2}	31	26	25	26	23	23	22	21
N_{TR}	37	35	32	31	29	29	27	27
Production-based TAC (€/kg)	2.391	2.339	2.215	2.193	2.179	2.168	2.161	2.153
CAPEX (M€/yr)	0.60	0.53	0.43	0.40	0.35	0.35	0.30	0.30
OPEX (M€/yr)	10.86	10.78	10.74	10.67	10.64	10.59	10.59	10.56

*Base case

Table A1: Antoine coefficients for component B as used in Multiflash for all case studies (see Appendix A1).

Antoine coefficient	**Value as used in Multiflash**
A_B	52.6
B_A-B_B – B_C – B_D	-6304.5
C_A-C_B – C_C – C_D	0
D_A-D_B – D_C – D_D	$8.9 \cdot 10^{18}$
E_A-E_B – E_C – E_D	-4.3
F_A-F_B – F_C – F_D	6
G_A-G_B – G_C – G_D	0
T_{min} (K)	273
T_{max} (K)	800

Table B1. Cost calculation correlations (in $) for standard distillation related capital costs taken from Coulson and Richardson (Sinnott and Towler 2020) based on 2007 costs.

Symbol ($)	Type of equipment	Additional information	Cost calculation
C_{DC}	Distillation column (shell) exl. heads, ports, internals etc	Vertical pressure vessel, Carpenter 20CB-3	$C_{DC} = 1.9\cdot(15000 + 68\cdot(W_{shell},kg)^{0.85})$ where from gPROMS ProcessBuilder: $W_{shell}(lb)=\pi\cdot(D_i+t_s)\cdot(L+0.8D_i)\cdot t_s\cdot d$ *(L is calculated using total number of stages and tray spacing)* $t_s=(t_p+t_w)/2$ $t_p=P_d\cdot D_i/(2\cdot S\cdot E-1.2\cdot P_d)$ $t_w=(0.22\cdot(D_o+18)\cdot L^2)/(S\cdot D_o^2)$ *(for symbols please see Notation list)*
C_{ST}	Column internals	Sieve trays, Carpenter 20CB-3 (for each tray)	$C_{ST} = 1.9\cdot(110 + 380\cdot(D_{tray},m)^{1.8})$
C_R	Reboiler	U-tube kettle reboiler[7]	$C_R = 25000 + 340\cdot(Q_{reboiler}/7500,m^2)^{0.9}$
C_C	Condenser	U-tube shell and tube[7]	$C_C = 24000 + 46\cdot(Q_{condenser}/7500,m^2)^{1.2}$
C_S	Stripper	Vertical pressure vessel, stainless steel	$C_S = 15000 + 68\cdot(W,kg)^{0.85}$
C_{RC}	Reactor	Jacketed, agitated, stainless steel	$C_{RC} = 53000+ 28000\cdot(V_R,m^3)^{0.8}$
C_{RD}	Reflux Drum	Cone roof tank	$C_{RD} = 5000+ 1400\cdot(V,m^3)^{0.7}$ *Volume based on 5 min residence time*

[7]The variable used in Table B1 for the calculation of reboiler and condenser cost, Q (W), is the heat duty required for the operation of each of these units. Q is divided (as $Q=U\cdot A\cdot\Delta T$) by the product of the heat transfer coefficient (750 $W/m^2\cdot K$) and temperature difference (10 K), i.e. 7500 W/m^2, to replace the surface area A (m^2) of the condenser/reboiler which is originally included in the cost calculation.

Table B2. Cost calculation correlations (in €/s) for standard distillation operating costs provided by Nouryon.

Symbol (€/s)	Type of operational cost	Cost calculation
C_{OS}	Steam	$C_{OS} = Q_{reboiler}(J/s) \cdot 24 \cdot 10^{-9}(€/J)$
C_{OF}	Feedstock	$C_{OF}=F_T\ (kg/s) \cdot 1(€/kg)$ FT=F1+F2+…+FN , where N is the number of feed streams
C_{OW}	Waste treatment	$C_{OW} = F_{OW}(kg/s) \cdot 0.22(€/kg_{organic})$
C_{main}	Plant maintenance	$C_{main}=(0.1 \cdot CAPEX_{2019})/(8000 \cdot 3600)$